Table 3. Demographics and clinical characteristics of HAM/TSP patients (Test Set).

	Total	Stable HAM/TSP	Deteriorating HAM/TSP	
	n = 23	n = 11	n = 9	*p*-value*
Demographics				
Age, y**	58 [22–75]	61 [22–75]	59 [48–68]	0.8491†
Female sex	78.3%	81.8%	77.8%	1.000‡
Clinical characteristics				
Age of onset, y**	43 [12–70]	40 [14–70]	51 [39–63]	0.0184†
Disease duration, y**	9 [2–41]	19 [5–41]	6 [2–14]	0.0148†
OMDS**	5 [2–8]	5 [4–8]	5 [4–8]	0.4526†

In the Test set, deteriorating patients experienced disease onset later in life and had been living with the disease for shorter periods, but there were no significant differences in current age or OMDS.
*Stable HAM/TSP vs Deteriorating HAM/TSP.
**Data are expressed as median [range].
†By Mann-Whitney test.
‡By Fisher's exact test.
OMDS = Osame's Motor Disability Score.
doi:10.1371/journal.pntd.0002479.t003

Classification system based on the natural history of HAM/TSP

The 53 total HAM/TSP patients without any history of HAM/TSP-targeting treatments were interviewed using a questionnaire (Figure S2) to determine the changes in Osame's Motor Disability Score (OMDS) over time (Figure S3). OMDS is a standardized neurological rating scale as a measure of disability [10] (Figure S1). Based on the changes in OMDS, "deteriorating cases" and "stable cases" were identified in both the Training set and Test set patient cohorts. Patients with deteriorating HAM/TSP were defined as those whose OMDS worsened ≥3 grades over four years and patients with stable HAM/TSP were defined as those whose OMDS remained unchanged or worsened 1 grade over four years. Patients whose OMDS worsened 2 grades over four years were excluded from the patient cohort in order to create a larger gap between the deteriorating and stable patient groups.

Statistical analysis

GraphPad Prism 5 (GraphPad Software, Inc., La Jolla, CA USA) was used to plot graphs and perform statistical analyses. Differences between the two subject groups were tested using the Mann-Whitney U-test. Receiver operating characteristic (ROC) analysis was performed to examine the sensitivity and specificity of individual biomarkers. For the ROC analyses, an area under the ROC curve (AUC) of 1.0 was used to represent a perfect test with 100% sensitivity and 100% specificity, whereas an area of 0.5 was used to represent random discrimination. Spearman's rank correlation test was employed to investigate the correlation between the four CSF markers (CXCL10, CXCL9, neopterin, and cell count) and the proviral load in PBMCs. To compare the four CSF markers between three groups (HTLV-1-infected control, n = 8; stable HAM/TSP, n = 25; and deteriorating HAM/TSP, n = 20), we used the Kruskal–Wallis test followed by Dunn's post-hoc tests. P-values<0.05 were considered statistically significant.

Results

Identification of biomarkers elevated in the blood of HAM/TSP patients

In order to identify candidate blood markers for HAM/TSP, the concentrations of IL-1β, TNF-α, and IFN-γ were measured in plasma samples from four ACs and four HAM/TSP patients. Plasma levels of IL-1β and TNFα were below the detection limits (<2.3 pg/mL and <1.2 pg/mL, respectively) except in one patient with HAM/TSP. Plasma IFN-γ levels showed no significant differences between ACs and HAM/TSP patients (median 10.4 pg/mL and 13.9 pg/mL, respectively). Therefore, these quantities were not measured in additional samples (Figure S1). The proviral DNA load in PBMCs, serum sIL-2R, and plasma levels of the chemokines CXCL9, CXCL10, CXCL11, and CCL5 were also measured in 22 ACs and 30 HAM/TSP patients without any history of immunomodulating treatments, including corticosteroids, IFN-α, and immunosuppressive drugs. The results revealed that serum levels of sIL-2R, plasma levels of CXCL10 and CXCL9, and proviral DNA load in PBMCs were markedly higher in HAM/TSP patients compared to ACs ($p \leq 0.0001$, Figure 1A). These quantities were then compared using ROC analysis to determine which parameters were superior markers for HAM/TSP. From the results of the ROC analysis, we determined that serum sIL-2R and plasma CXCL10 had the highest potential for distinguishing HAM/TSP patients from ACs with high sensitivity and specificity (area under the ROC curve [AUC]>0.9), followed by plasma CXCL9 and HTLV-1 proviral load in PBMCs (0.8<AUC<0.9) (Figure 1B). Thus, four candidate blood biomarkers were selected for further investigation: serum sIL-2R, plasma CXCL10, plasma CXCL9, and HTLV-1 proviral load in PBMCs.

Identification of biomarkers elevated in the CSF of HAM/TSP patients

In order to identify candidate CSF markers for HAM/TSP, elevated levels of various potential markers were screened for in CSF samples from HAM/TSP patients. CSF IL-17A was detectable (>3.0 pg/mL) in only one of eight HAM/TSP patients screened (including six deteriorating-type patients), and the level in this one patient (deteriorating-type) was negligible (4.0 pg/mL). CSF IFN-γ was detectable (>1.8 pg/mL) in only 3 of 10 HAM/TSP patients screened (six deteriorating patients), and the levels in all three were negligible (range 3.3–4.2 pg/mL). Therefore, these cytokines were not measured in additional patients. Total protein, cell count, IgG, neopterin, sIL-2R, and nine chemokines (CXCR3 ligands: CXCL9, CXCL10, and CXCL11; CCR5 ligands: CCL3, CCL4, and CCL5; CCR4 ligands: CCL17 and CCL22; CCR6

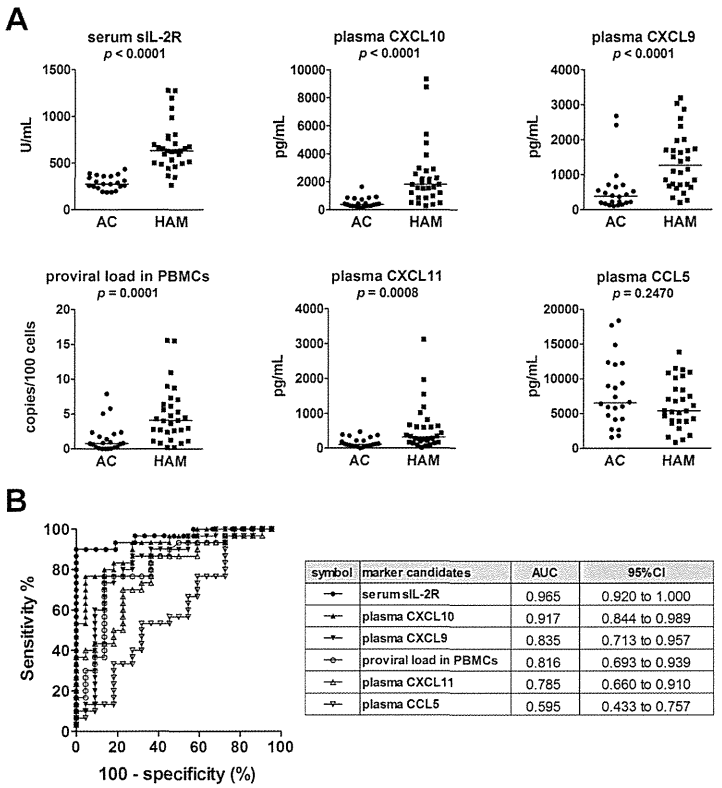

symbol	marker candidates	AUC	95%CI
	serum sIL-2R	0.965	0.920 to 1.000
	plasma CXCL10	0.917	0.844 to 0.989
	plasma CXCL9	0.835	0.713 to 0.957
	proviral load in PBMCs	0.816	0.693 to 0.939
	plasma CXCL11	0.785	0.660 to 0.910
	plasma CCL5	0.595	0.433 to 0.757

Figure 1. Selection of candidate biomarkers in the blood by comparing HAM/TSP patients and asymptomatic carriers. (**A**) Serum levels of soluble IL-2 receptor (sIL-2R), proviral loads in peripheral blood mononuclear cells (PBMCs), and plasma levels of four chemokines (chemokine (C-X-C motif) ligand (CXCL) 9, CXCL10, CXC11, and chemokine (C-C motif) ligand (CCL) 5) were compared between HAM/TSP patients (HAM; n = 30) and asymptomatic carriers (AC; n = 22). Horizontal bars indicate the median values. The Mann-Whitney *U*-test was used for statistical analysis. (**B**) Receiver operating characteristic (ROC) analysis was employed to assess the sensitivities and specificities of the six markers exhibited in part (A) for discriminating HAM/TSP patients from ACs: greater proximity of the ROC curve to the upper left corner indicates higher sensitivity and specificity of the marker. AUC = area under the ROC curve; 95% CI = 95% confidence interval.
doi:10.1371/journal.pntd.0002479.g001

ligand: CCL20) were also measured in the CSF of 30 untreated HAM/TSP patients and in eight HTLV-1-infected control subjects (seven ACs and one patient with smoldering ATL). The results indicated that CSF levels of CXCL10, neopterin, and CXCL9 were remarkably higher in HAM/TSP patients compared to control subjects ($p<0.0001$ overall, Figures 2A and S4) and that CSF levels of cell count and CCL5 were less so but still significantly higher ($p = 0.0019$ and $p = 0.0119$, respectively; Figure 2A). By contrast, there were no differences in the CSF levels of IgG and total protein between HAM/TSP patients and control subjects, and CSF sIL-2R levels were only detectable in a single HAM/TSP patient (data not shown). ROC analysis showed that the CSF levels of CXCL10, neopterin, CXCL9, and CSF cell count could be used to relatively accurately distinguish HAM/TSP patients from control subjects (AUC>0.8) (Figure 2B). Therefore, these four CSF markers were selected as candidates for further investigation. It should be noted that the sensitivity of CSF cell count was very low (36.7%) when compared to the other three: CXCL10 (83.3%), CXCL9 (86.7%), and neopterin (76.7%) (Figure S5).

Identification of biomarkers correlated with rate of HAM/TSP disease progression

In short, we selected nine markers: eight markers chosen based on the analyses described above and CSF anti-HTLV-1 antibody titer, which is a known diagnostic marker for HAM/TSP. To determine which biomarkers were associated with HAM/TSP disease progression, the levels of these nine markers were compared between the deteriorating and stable HAM/TSP patient groups (see Methods for definitions of deteriorating and stable). The results revealed that all five CSF markers were significantly higher in the deteriorating group compared to the stable group (Figure 3A), but that none of the four blood markers, including proviral load, were significantly different between the two groups. The deteriorating group included three patients with particularly rapidly progressive HAM/TSP, defined as those who had been confined to wheelchairs (OMDS: ≥ grade 6) within two years after the onset of symptoms [13,14] (black circles in Figures 3A and S3B). These rapid progressors exhibited high levels of the CSF markers and high proviral loads. ROC analysis revealed that the levels of the CSF markers (CXCL10, CXCL9, neopterin, and cell count), but not anti-HTLV-1 antibody titer, distinguished clearly between patients with deteriorating HAM/TSP and stable HAM/TSP (AUC>0.8, Figure 3B).

Validation of nine candidate biomarkers using the Test Set

To validate the results obtained using the Training Set, the same nine markers were compared between deteriorating and stable patients using the Test Set (a second cohort of 23 HAM/

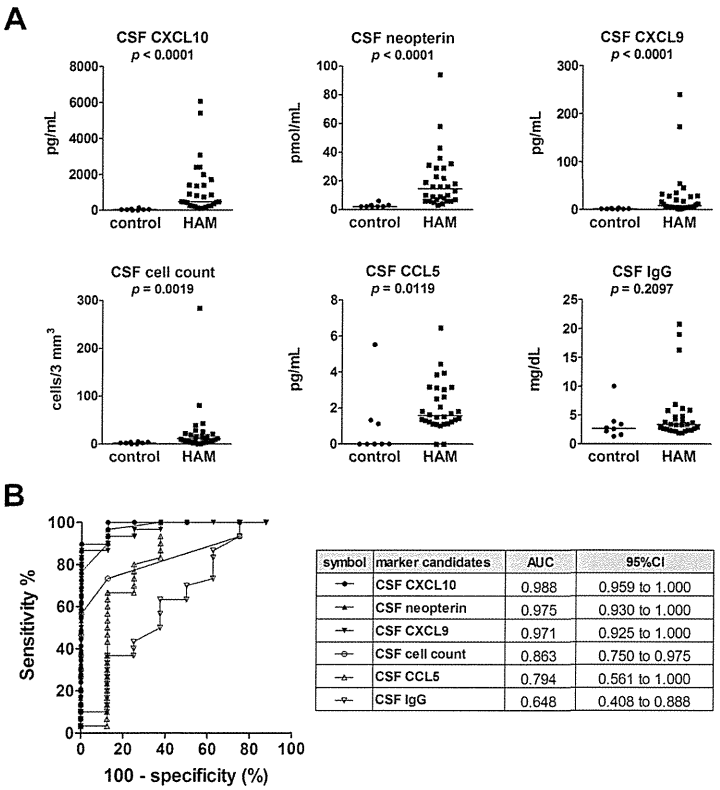

symbol	marker candidates	AUC	95%CI
	CSF CXCL10	0.988	0.959 to 1.000
	CSF neopterin	0.975	0.930 to 1.000
	CSF CXCL9	0.971	0.925 to 1.000
	CSF cell count	0.863	0.750 to 0.975
	CSF CCL5	0.794	0.561 to 1.000
	CSF IgG	0.648	0.408 to 0.888

Figure 2. Selection of candidate biomarkers in the cerebrospinal fluid (CSF) by comparing HAM/TSP patients and control subjects. (**A**) CSF levels of total protein, cell count, IgG, neopterin, sIL-2R, and nine chemokines (CCL3, CCL4, CCL5, CXCL9, CXCL10, CXC11, CCL17, CCL20, and CCL22) were measured and compared between HAM/TSP patients (HAM; n = 30) and HTLV-1-infected control subjects (control; n = eight: seven ACs and one ATL patient). Data is shown for the top six CSF markers ranked according to the significance of the difference between the HAM/TSP patients and the control subjects. Horizontal bars indicate the median values. The Mann-Whitney *U*-test was used for statistical analysis. (**B**) ROC analysis was employed to assess the sensitivities and specificities of the six markers exhibited in part (A) for discriminating HAM/TSP patients from controls. AUC = area under the ROC curve; 95% CI = 95% confidence interval.
doi:10.1371/journal.pntd.0002479.g002

TSP patients that had not undergone HAM/TSP-targeting treatment). As shown in Figure 4A, the results indicated that the levels of five CSF markers, proviral load in PBMCs, and serum sIL-2R were significantly higher in deteriorating cases than in stable cases. Among them, CSF levels of CXCL10, CXCL9, neopterin, and CSF cell count exhibited particularly high sensitivities and specificities for detecting the deteriorating HAM/TSP cases in the Test set as well as Training set (AUC>0.8, Figures 4B and S1).

Demographic and clinical characteristics of the subjects

The demographics of the HAM/TSP patients versus the control subjects for both the blood tests and CSF analyses were compared and evaluated for statistical significance (Table S1). There were no significant differences in age or gender distribution between the HAM/TSP patients and either control subject group.

Similarly, the demographic and clinical characteristics of stable versus deteriorating HAM/TSP subjects in both the Training and Test sets are shown in Tables 2 and 3, respectively. There were no significant differences in age or gender distribution among either set, but deteriorating patients in both sets were significantly older at disease onset and had been living with the disease for shorter periods of time. Deteriorating patients in the Training set scored higher OMDS values than their stable counterparts ($p<0.01$), but there was no such significant difference in the Test set.

To investigate the potential influence of disease duration as a secondary variable, a new test group was created containing only those patients for whom the disease onset date was 7–13 years prior to the sample collection day. Patients fitting this criterion were selected from the 53 total available from both the Training and Test sets: eight stable patients and ten deteriorating patients; we confirmed that there was no significant difference in disease duration between these two groups. The results remained consistent with our previous findings: CSF CXCL10, CXCL9, and neopterin were all elevated in deteriorating patients with respect to stable patients ($p<0.01$, Figure 5).

Follow-up mini-study on biomarker levels over time

Four stable HAM/TSP patients were left completely untreated and followed for a period of three to five years. Within this time, one patient rose one grade on the OMDS scale, and the other three experienced no change in OMDS grade at all. The levels of CSF CXCL10 and neopterin remained consistently low over time (Figure S6).

Discussion

To date, there have been few well-designed studies that have evaluated the relationship between biomarkers and HAM/TSP disease progression. In a previous retrospective study with 100 untreated HAM/TSP patients, a significant association was

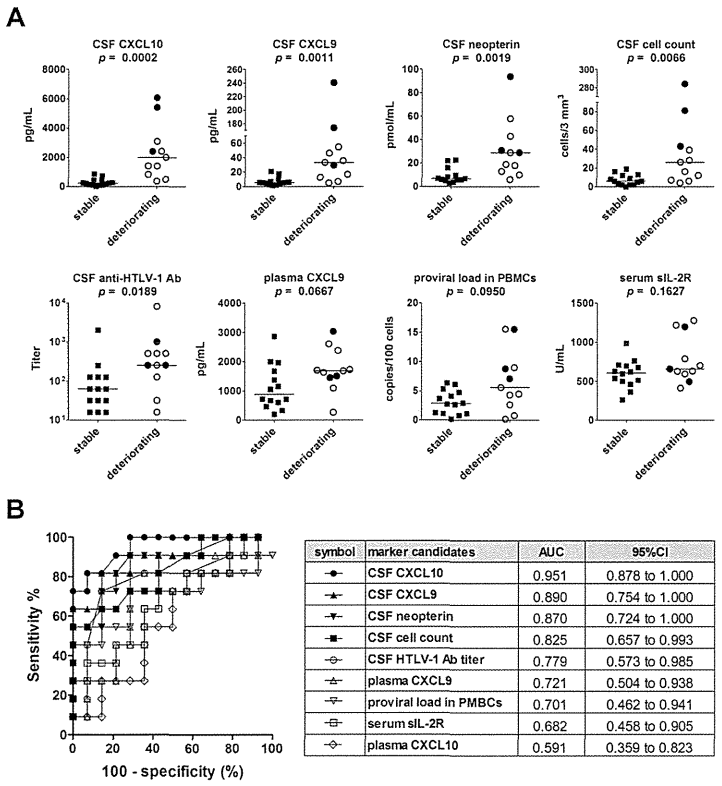

symbol	marker candidates	AUC	95%CI
	CSF CXCL10	0.951	0.878 to 1.000
	CSF CXCL9	0.890	0.754 to 1.000
	CSF neopterin	0.870	0.724 to 1.000
	CSF cell count	0.825	0.657 to 0.993
	CSF HTLV-1 Ab titer	0.779	0.573 to 0.985
	plasma CXCL9	0.721	0.504 to 0.938
	proviral load in PMBCs	0.701	0.462 to 0.941
	serum sIL-2R	0.682	0.458 to 0.905
	plasma CXCL10	0.591	0.359 to 0.823

Figure 3. Identification of biomarkers associated with clinical progression of HAM/TSP. (**A**) Five CSF marker candidates (CXCL10, CXCL9, neopterin, cell count, and anti-HTLV-1 antibody titer) and four blood marker candidates (proviral load in PBMCs, serum sIL-2R, plasma CXCL9, and plasma CXCL10) were compared among a cohort of patients called the Training Set (deteriorating HAM/TSP, n = 11; stable HAM/TSP, n = 14). Data is shown for the top eight CSF markers ranked according to the significance of the difference between the deteriorating and stable subjects. Black circles indicate patients with particularly rapidly progressive HAM/TSP. Horizontal bars indicate the median values. The Mann-Whitney *U*-test was used for statistical analysis. (**B**) ROC analysis was employed to assess the sensitivities and specificities of the nine markers listed above for discriminating deteriorating HAM/TSP patients from stable patients. AUC = area under the ROC curve; 95% CI = 95% confidence interval.
doi:10.1371/journal.pntd.0002479.g003

demonstrated to exist between higher HTLV-1 proviral load in PBMCs and poor long-term prognosis; however, the predictive value of high proviral load appeared to be too low to qualify it as a marker for disease progression in clinical practice [32]. Here we conducted a retrospective study to compare for the first time the relationships of PBMC proviral load and several inflammatory biomarker candidates to disease progression in untreated HAM/TSP patients.

In this study, elevated CSF cell count, neopterin concentration, and CSF levels of CXCL9 and CXCL10 were well-correlated with disease progression over the four year period under study, better even than HTLV-1 proviral load in PBMCs (Figures 3 and 4). As CSF pleocytosis, CSF CXCL10, CSF CXCL9, and CSF neopterin are known indicators of inflammation in the central nervous system [33,34], our findings indicate that the rate of HAM/TSP progression is more closely reflected by the amount of inflammatory activity in the spinal cord than by the PBMC proviral load. However, we also found a significant correlation between PBMC proviral load and the levels of the CSF markers identified in this study (Figure S7), indicating that a higher PBMC proviral load does indeed suggest more inflammation in the spinal cord and therefore a poorer long-term prognosis. These findings are consistent with the theory that HAM/TSP is the result of an excess of inflammatory mediators caused by the presence of HTLV-1-infected T-cells [35–37].

The HTLV-1 proviral load in the CSF as well as the ratio of the proviral load in the CSF to that in PBMCs have been reported to be effective for discriminating HAM/TSP patients from ACs or multiple sclerosis patients infected with HTLV-1 [38,39]. Some researchers have suggested that these values might be associated with the rate of disease progression, but there has been only one small cohort study and one case report investigating this point, and so the significance of this experimental evidence is still questionable [40,41]. In addition to statistical validation with multiple, larger cohorts, it would also be beneficial to use precise definitions for progressive versus stable patients, as we have done in this study. Although the volume of CSF available per sample was too limited to measure CSF proviral load in the present study, we plan to incorporate CSF proviral load in a future prospective study and compare its usefulness to that of other biomarker candidates.

From our results, we concluded that of the potential biomarkers under study, CXCL10, CXCL9, and neopterin are the most fit for determining the level of spinal cord inflammation, and thus the most fit for predicting disease progression in HAM/TSP patients. Although the CSF cell count is an easily measurable inflammatory marker, it is not sensitive enough to reliably detect the level of spinal cord inflammation. Numerous patients with CSF cell counts within the normal range exhibited high levels of other inflammatory markers, such as neopterin and CXCL10 (Figure S5). In fact, it has been reported that CSF pleocytosis is present in only approximately 30% of HAM/TSP patients [42]. Furthermore, in

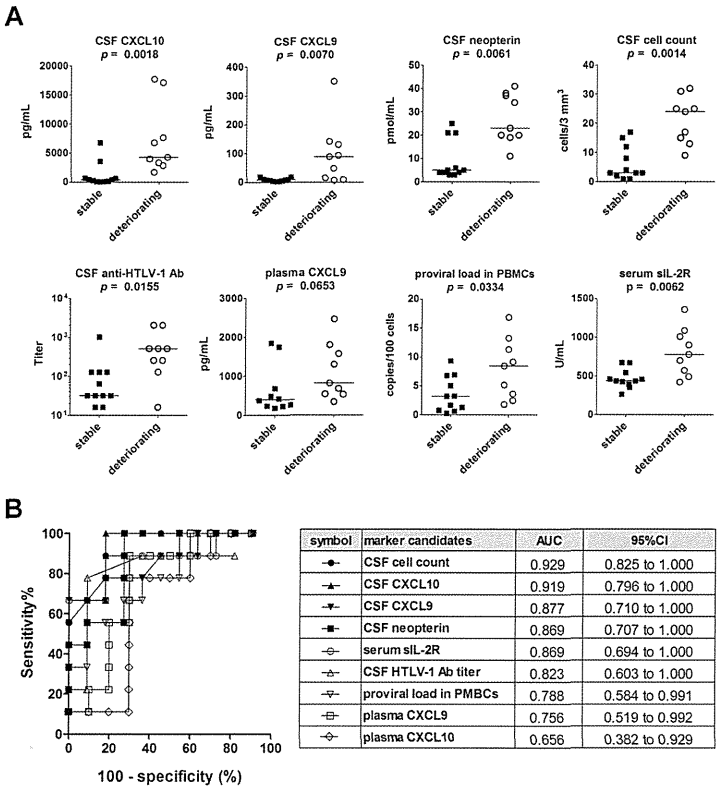

symbol	marker candidates	AUC	95%CI
	CSF cell count	0.929	0.825 to 1.000
	CSF CXCL10	0.919	0.796 to 1.000
	CSF CXCL9	0.877	0.710 to 1.000
	CSF neopterin	0.869	0.707 to 1.000
	serum sIL-2R	0.869	0.694 to 1.000
	CSF HTLV-1 Ab titer	0.823	0.603 to 1.000
	proviral load in PMBCs	0.788	0.584 to 0.991
	plasma CXCL9	0.756	0.519 to 0.992
	plasma CXCL10	0.656	0.382 to 0.929

Figure 4. Validation of potential markers using the Test Set. (**A**) Five CSF marker candidates (CXCL10, CXCL9, neopterin, cell count, and anti-HTLV-1 antibody titer) and four blood marker candidates (proviral load in PBMCs, serum sIL-2R, plasma CXCL9, and plasma CXCL10) were compared among a second cohort of patients called the Test Set (deteriorating HAM/TSP, n = 9; stable HAM/TSP, n = 11). Data is shown for the top eight CSF markers ranked according to the significance of the difference between the deteriorating and stable subjects. Horizontal bars indicate the median values. The Mann-Whitney *U*-test was used for statistical analysis. (**B**) ROC analysis was employed to assess the sensitivities and specificities of the nine markers listed above for discriminating deteriorating HAM/TSP patients from stable patients. AUC = area under the ROC curve; 95% CI = 95% confidence interval.
doi:10.1371/journal.pntd.0002479.g004

our study, there was no significant difference in CSF cell count between the control subjects and the stable HAM/TSP patients (Figure S8).

We also explored the possibility of combining multiple biomarkers via multiple logistic regression to form a combination more sensitive and specific than individual markers, but the results indicated that there is not much to be gained from combinations (data not shown).

While there were no significant demographic differences between subject groups, the clinical characteristics of stable versus deteriorating HAM/TSP patients of course differed widely (Tables 2, 3, and S2). We confirmed the already well-reported statistic that deteriorating patients experience HAM/TSP onset relatively late in life [12,14,20] ; our data also reflected the short disease duration expected of deteriorating patients, who by definition progress through the disease more rapidly than their stable counterparts. As patients in all groups were of similar age at sample collection, the significant difference in age of onset should not have any impact on our findings. However, it was necessary to consider the possibility that those patients in a later stage of the disease (i.e. those listed with longer disease durations) might possess elevated or diminished biomarker levels regardless of rate of disease progression. We confirmed that this difference in disease duration was not a confounding factor in our selection of candidate biomarkers by comparing stable and deteriorating HAM/TSP patients with similar disease durations (7–13 years), and we were able to obtain results consistent with our earlier findings (Figure 5). Finally, the OMDS values for the stable and deteriorating patient groups in the Test set were perfectly identical, eliminating the need to consider the possibility that the biomarkers could have been elevated according to disease severity regardless of rate of progression.

The main limitation of our retrospective study is that our samples were collected from patients at the end of the four year period during which the extent of progression was analyzed as opposed to the beginning of the four year period, which would have been optimal for directly measuring their prognostic powers. Of course, the patients with severe HAM/TSP symptoms began undergoing treatment soon after sample collection, rendering any observations on disease course after sample collection un-useable for analysis in this study. While this situation is non-ideal, we hypothesize that biomarker levels in a given patient do not substantially change over a few years' time. We were actually able to monitor the biomarker levels of four untreated HAM/TSP patients over 3–5 years, and the levels remained relatively stable in all four subjects over time (Figure S6), supporting our hypothesis. However, these were all stable HAM/TSP patients (hence the lack of treatment), and so we cannot rule out the possibility that biomarker levels in untreated deteriorating patients may dramatically rise, fall, or fluctuate. The results of the analysis of patients with similar disease durations (Figure 5) also support our hypothesis that disease duration is not an important determinant

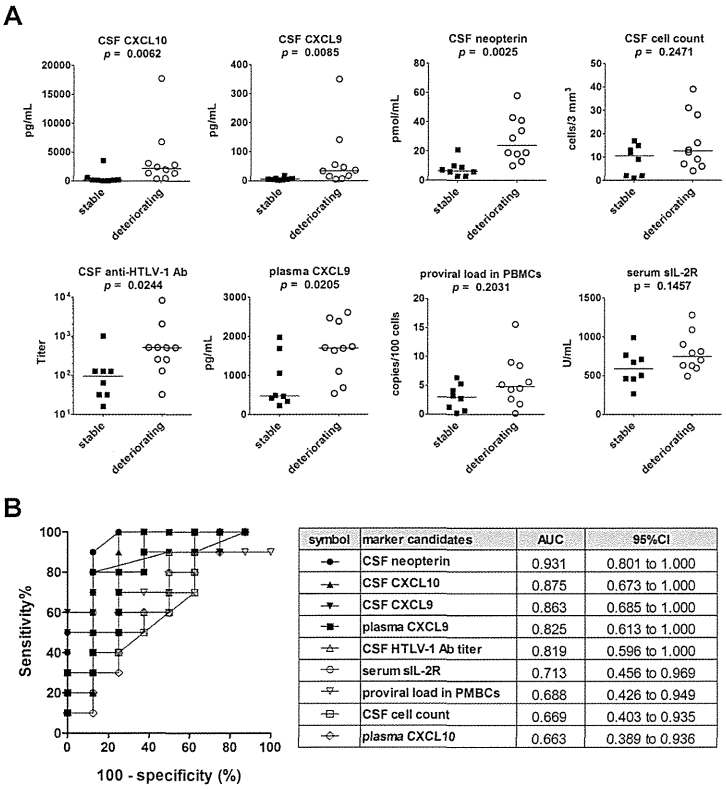

symbol	marker candidates	AUC	95%CI
	CSF neopterin	0.931	0.801 to 1.000
	CSF CXCL10	0.875	0.673 to 1.000
	CSF CXCL9	0.863	0.685 to 1.000
	plasma CXCL9	0.825	0.613 to 1.000
	CSF HTLV-1 Ab titer	0.819	0.596 to 1.000
	serum sIL-2R	0.713	0.456 to 0.969
	proviral load in PMBCs	0.688	0.426 to 0.949
	CSF cell count	0.669	0.403 to 0.935
	plasma CXCL10	0.663	0.389 to 0.936

Figure 5. Comparison of potential markers in stable and deteriorating HAM/TSP patients with similar disease durations. (**A**) Five CSF marker candidates (CXCL10, CXCL9, neopterin, cell count, and anti-HTLV-1 antibody titer) and four blood marker candidates (proviral load in PBMCs, serum sIL-2R, plasma CXCL9, and plasma CXCL10) were compared among all patients from both the Training and Test Sets pooled together with similar disease durations (range: 7–13 years; no significant difference in duration between stable (n = 8) and deteriorating (n = 10) groups). Data is shown for the top eight CSF markers ranked according to the significance of the difference between the deteriorating and stable subjects. Horizontal bars indicate the median values. The Mann-Whitney *U*-test was used for statistical analysis. (**B**) ROC analysis was employed to assess the sensitivities and specificities of the nine markers listed above for discriminating deteriorating HAM/TSP patients from stable patients while controlling for disease duration. AUC = area under the ROC curve; 95% CI = 95% confidence interval.
doi:10.1371/journal.pntd.0002479.g005

of biomarker levels, but it is of course not conclusive. We expect that a prospective study in the future will reveal the answer to this question.

The results of this study indicate that CXCL9 and/or CXCL10 may play a key role in the pathogenesis of HAM/TSP by recruiting more inflammatory cells to the spinal cord lesions. In this study, we measured the levels of the chemokines in the CSF that might play a part in inducing the migration of T-helper (Th) cells. $CD4^+$ Th cells differentiate from naïve T-cells to members of the Th subset (e.g., Th1, Th2, Th17, or Treg cells), and each one expresses its own characteristic chemokine receptors [43]. Usually, Th1 cell express CCR5/CXCR3 receptors, Th2 and Treg cells express CCR4, and Th17 express CCR6. Interestingly, CCR4 ligands (CCL17 and, CCL22) and the CCR6 ligand (CCL20) were not detected in the CSF of HAM/TSP patients. Moreover, of the CCR5 ligands, only CCL5 was elevated, but only slightly, and there was no association with rate of disease progression. Of the CXCR3 ligands, only CXCL9 and CXCL10 were correlated with the rate of disease progression. These results show that the pathology of HAM/TSP is unique among immune disorders in that, unlike other inflammatory disorders such as multiple sclerosis or rheumatoid arthritis that exhibit Th17 as well as Th1 involvement, the chemokine involvement in HAM/TSP is Th1-dominant. In a previous study, cytokines produced by HTLV-1-infected T-cells in HAM/TSP patients were analyzed, and the results showed that IFN-γ was elevated and IL-17 reduced [43,44]. Taken together, the results of these studies indicate that the characteristics of HTLV-1-infected T-cells themselves may be responsible for the Th1-dominant chemokine production observed in HAM/TSP. Also, these results suggest that the CXCR3-ligand (CXCL9 and CXCL10) interactions play an important role in the pathophysiology of HAM/TSP. Recently it was established that these CXCR3-ligand interactions are extremely important for the pathogenesis of several neurological disorders [33]. Therefore, future research on the significance of these interactions in the pathogenic process of HAM/TSP will be important for clarifying the suitability of CXCL9 and CXCL10 as biomarkers or therapeutic targets.

In conclusion, in this retrospective study, we have demonstrated that CSF levels of CXCL10, CXCL9, and neopterin are promising candidate prognostic biomarkers for HAM/TSP. These biomarkers may provide a means for the early identification of patients at increased risk of debilitating disease progression, those that may need anti-inflammatory therapies to limit or prevent this, and for evaluating the efficacy of such therapies. This initial identification of prognostic biomarkers for HAM/TSP should be followed by a future multicenter prospective clinical study.

Supporting Information

Figure S1 Diagram illustrating the biomarker selection process. A total of 26 biomarker candidates including 9 in the blood and 17 in the CSF underwent the following selection processes: 1) pre-screening of the cytokines for presence in HAM/TSP patients, 2) selection for markers elevated in HAM/TSP patients with respect to controls (AUC>0.8), 3) selection for markers elevated in deteriorating HAM/TSP patients with respect to stable patients (AUC>0.8) in a cohort termed the Training Set, 4) validation of the selected markers by evaluating again (AUC>0.8) in a second cohort termed the Test Set. The darkening of an arrow's color represents that marker's failure to meet the selection criteria, and the termination of an arrow indicates that no further testing was conducted for that marker. CYT = cytokine, HTLV-1 PVL = HTLV-1 proviral load, Ab Titer = anti-HTLV-1 antibody titer, AUC = area under the ROC curve.
(TIF)

Figure S2 Questionnaire on the development of motor disability over time as measured using Osame's Motor Disability Score (OMDS). The first and second columns indicate the OMDS numerical value and description, respectively. Doctors interviewed the patients and filled in the table according to the following instructions: in the bottom row, write the ages at which symptoms listed to the left first appeared, and above the age check the box in the row corresponding to the symptom.
(TIF)

Figure S3 Rate of disease progression in HAM/TSP patients without any history of HAM/TSP-targeting treatment. Each line illustrates the change in OMDS over time for an individual patient after disease onset for (**A**) all patients in the Training Set (n = 30) and (**B, left**) only deteriorating patients (n = 11) including three particularly rapidly progressive patients (shown as solid black circles) and (**B, right**) only stable patients (n = 14).
(TIF)

Figure S4 Comparison of CSF levels of nine chemokines in control subjects and HAM/TSP patients. The CSF levels of nine chemokines (CCR5 ligands: CCL3, CCL4, and CCL5; CXCR3 ligands: CXCL9, CXCL10, and CXCL11; CCR4 ligands: CCL17 and CCL22; CCR6 ligand: CCL20) were compared between control subjects (control; n = 8) and HAM/TSP patients (HAM; n = 30). Horizontal bars indicate median values. The Mann-Whitney *U*-test was used for statistical analysis.
(TIF)

Figure S5 Low sensitivity of CSF cell count for detection of HAM/TSP. (**A**) Sensitivities of four potential CSF markers for detection of HAM/TSP. For CSF CXCL10, CXCL9, and neopterin, dotted lines indicate reference values, defined as mean for control subjects +3 standard deviations. For CSF cell count, the dotted line represents the pre-established reference value of 15/3 mm^3. The sensitivity of CSF cell count was much lower than those of the other CSF markers. (**B**) Direct comparison of the sensitivities of CSF cell count and the other three CSF markers. The horizontal dotted lines all represent the reference value for CSF cell count ($\leq$15/3 mm^3), and each vertical dotted line indicates the reference value for each of the other CSF markers. With these lines drawn, one can see in the shaded area the numerous patients with CSF cell counts within the normal range but abnormally high levels of each of the other inflammatory markers, thus directly illustrating the comparatively low sensitivity of CSF cell count.
(TIF)

Figure S6 Changes in levels of CSF markers and OMDS over time in four untreated HAM/TSP patients. The three graphs illustrate the changes over time in CSF CXCL10 (top), neopterin (middle), and OMDS (bottom) for four untreated stable HAM/TSP patients. The patients were observed for 60 months (No. 1), 56 months (No. 2), 49 months (No. 3), and 39 months (No. 4).
(TIF)

Figure S7 Significant positive correlation between the proviral load in PBMCs and four CSF markers. HTLV-1 proviral load in PBMCs was compared with the levels of each of four CSF markers (CXCL10, CXCL9, neopterin, and cell count) in HAM/TSP patients (n = 53). Data analysis was performed using the Spearman's rank correlation test.
(TIF)

Figure S8 Significant higher CSF levels of CXCL10, CXCL9, and neopterin even in stable HAM/TSP compared to controls. The levels of four CSF markers (CXCL10, CXCL9, neopterin, and cell count) were compared among three groups (HTLV-1-infected controls, n = 8; stable HAM/TSP patients, n = 25; and deteriorating HAM/TSP patients, n = 20) assembling patients from both Training and Test Sets combined. The horizontal bar indicates the median value for each group. Statistical analysis was performed using the Kruskal–Wallis test followed by Dunn's post-hoc tests. ns: not significant, * $P<0.05$, *** $P<0.001$.
(TIF)

Table S1 Demographics of HAM/TSP patients and control subjects. There were no significant differences in the demographics of HAM/TSP patients versus control subjects.
(DOCX)

Table S2 Demographics and clinical characteristics of HAM/TSP patients (Training set + Test Set). Among the HAM/TSP patients from the Training and Test Sets pooled together, deteriorating patients experienced disease onset significantly later in life and had lived with the disease for shorter periods.
(DOCX)

Acknowledgments

We thank K. Takahashi, Y. Kunitomo, Y. Sato, Y. Hasegawa, M. Koike, Y. Suzuki-Ishikura, and A. Une for technical assistance.

Author Contributions

Conceived and designed the experiments: YY TS SJ SI. Performed the experiments: TS HA NA JY. Analyzed the data: TS AU NA NY HA JY EI TU YH KN TN. Contributed reagents/materials/analysis tools: YY AU YH. Wrote the paper: YY TS ACR.

References

1. Poiesz BJ, Ruscetti FW, Gazdar AF, Bunn PA, Minna JD, et al. (1980) Detection and isolation of type C retrovirus particles from fresh and cultured lymphocytes of a patient with cutaneous T-cell lymphoma. Proc Natl Acad Sci USA 77: 7415–7419.
2. Yamaguchi K, Watanabe T (2002) Human T lymphotropic virus type-I and adult T-cell leukemia in Japan. Int J Hematol 76 Suppl 2: 240–245.
3. Murphy EL, Hanchard B, Figueroa JP, Gibbs WN, Lofters WS, et al. (1989) Modelling the risk of adult T-cell leukemia/lymphoma in persons

infected with human T-lymphotropic virus type I. Int J Cancer 43: 250–253.
4. Kaplan JE, Osame M, Kubota H, Igata A, Nishitani H, et al. (1990) The risk of development of HTLV-I-associated myelopathy/tropical spastic paraparesis among persons infected with HTLV-I. J Acquir Immune Defic Syndr 3: 1096–1101.
5. Maloney EM, Cleghorn FR, Morgan OS, Rodgers-Johnson P, Cranston B, et al. (1998) Incidence of HTLV-I-associated myelopathy/tropical spastic paraparesis (HAM/TSP) in Jamaica and Trinidad. J Acquir Immune Defic Syndr Hum Retrovirol 17: 167–170.
6. Orland JR, Engstrom J, Fridey J, Sacher RA, Smith JW, et al. (2003) Prevalence and clinical features of HTLV neurologic disease in the HTLV Outcomes Study. Neurology 61: 1588–1594.
7. Proietti FA, Carneiro-Proietti AB, Catalan-Soares BC, Murphy EL (2005) Global epidemiology of HTLV-I infection and associated diseases. Oncogene 24: 6058–6068.
8. Gessain A, Cassar O (2012) Epidemiological Aspects and World Distribution of HTLV-1 Infection. Front Microbiol 3: 388.
9. Casseb J (2009) Is human T cell lymphotropic type 1 (HTLV-1)-associated myelopathy/tropical spastic paraparesis (HAM/TSP) syndrome a neglected disease? PLoS Negl Trop Dis 3: e487.
10. Osame M (1990) Review of WHO Kagoshima meeting and diagnostic guidelines for HAM/TSP. In: Blattner WA, editor. Human Retrovirology: HTLV. New York: Raven Press. pp. 191–197.
11. Gessain A, Barin F, Vernant JC, Gout O, Maurs L, et al. (1985) Antibodies to human T-lymphotropic virus type-I in patients with tropical spastic paraparesis. Lancet 2: 407–410.
12. Matsuzaki T, Nakagawa M, Nagai M, Usuku K, Higuchi I, et al. (2001) HTLV-I proviral load correlates with progression of motor disability in HAM/TSP: analysis of 239 HAM/TSP patients including 64 patients followed up for 10 years. J Neurovirol 7: 228–234.
13. Martin F, Fedina A, Youshya S, Taylor GP (2010) A 15-year prospective longitudinal study of disease progression in patients with HTLV-1 associated myelopathy in the UK. J Neurol Neurosurg Psychiatry 81: 1336–1340.
14. Olindo S, Cabre P, Lézin A, Merle H, Saint-Vil M, et al. (2006) Natural history of human T-lymphotropic virus 1-associated myelopathy: a 14-year follow-up study. Arch Neurol 63: 1560–1566.
15. Yamano Y, Sato T (2012) Clinical pathophysiology of human T-lymphotropic virus-type 1-associated myelopathy/tropical spastic paraparesis. Front Microbiol 3: 389.
16. Nagai M, Usuku K, Matsumoto W, Kodama D, Takenouchi N, et al. (1998) Analysis of HTLV-I proviral load in 202 HAM/TSP patients and 243 asymptomatic HTLV-I carriers: high proviral load strongly predisposes to HAM/TSP. J Neurovirol 4: 586–593.
17. Yamaguchi K, Nishimura Y, Kiyokawa T, Takatsuki K (1989) Elevated serum levels of soluble interleukin-2 receptors in HTLV-I-associated myelopathy. J Lab Clin Med 114: 407–410.
18. Nomoto M, Utatsu Y, Soejima Y, Osame M (1991) Neopterin in cerebrospinal fluid: a useful marker for diagnosis of HTLV-I-associated myelopathy/tropical spastic paraparesis. Neurology 41: 457.
19. Ali A, Rudge P, Dalgleish AG (1992) Neopterin concentrations in serum and cerebrospinal fluid in HTLV-I infected individuals. J Neurol 239: 270–272.
20. Nakagawa M, Izumo S, Ijichi S, Kubota H, Arimura K, et al. (1995) HTLV-I-associated myelopathy: analysis of 213 patients based on clinical features and laboratory findings. J Neurovirol 1: 50–61.
21. Kuroda Y, Matsui M, Takashima H, Kurohara K (1993) Granulocyte-macrophage colony-stimulating factor and interleukin-1 increase in cerebrospinal fluid, but not in serum, of HTLV-I-associated myelopathy. J Neuroimmunol 45: 133–136.
22. Kuroda Y, Matsui M (1993) Cerebrospinal fluid interferon-gamma is increased in HTLV-I-associated myelopathy. J Neuroimmunol 42: 223–226.
23. Nakamura S, Nagano I, Yoshioka M, Shimazaki S, Onodera J, et al. (1993) Detection of tumor necrosis factor-alpha-positive cells in cerebrospinal fluid of patients with HTLV-I-associated myelopathy. J Neuroimmunol 42: 127–130.
24. Umehara F, Izumo S, Ronquillo AT, Matsumuro K, Sato E, et al. (1994) Cytokine expression in the spinal cord lesions in HTLV-I-associated myelopathy. J Neuropathol Exp Neurol 53: 72–77.
25. Narikawa K, Fujihara K, Misu T, Feng J, Fujimori J, et al. (2005) CSF-chemokines in HTLV-I-associated myelopathy: CXCL10 up-regulation and therapeutic effect of interferon-alpha. J Neuroimmunol 159: 177–182.
26. Guerreiro JB, Santos SB, Morgan DJ, Porto AF, Muniz AL, et al. (2006) Levels of serum chemokines discriminate clinical myelopathy associated with human T lymphotropic virus type 1 (HTLV-1)/tropical spastic paraparesis (HAM/TSP) disease from HTLV-1 carrier state. Clin Exp Immunol 145: 296–301.
27. Tanaka M, Matsushita T, Tateishi T, Ochi H, Kawano Y, et al. (2008) Distinct CSF cytokine/chemokine profiles in atopic myelitis and other causes of myelitis. Neurology 71: 974–981.
28. Tattermusch S, Skinner JA, Chaussabel D, Banchereau J, Berry MP, et al. (2012) Systems biology approaches reveal a specific interferon-inducible signature in HTLV-1 associated myelopathy. PLoS Pathog 8: e1002480.
29. Nagai M, Kubota R, Greten TF, Schneck JP, Leist TP, et al. (2001) Increased activated human T cell lymphotropic virus type I (HTLV-I) Tax11-19-specific memory and effector CD8+ cells in patients with HTLV-I-associated myelopathy/tropical spastic paraparesis: correlation with HTLV-I provirus load. J Infect Dis 183: 197–205.
30. Yamano Y, Nagai M, Brennan M, Mora CA, Soldan SS, et al. (2002) Correlation of human T-cell lymphotropic virus type 1 (HTLV-1) mRNA with proviral DNA load, virus-specific CD8(+) T cells, and disease severity in HTLV-1-associated myelopathy (HAM/TSP). Blood 99: 88–94.
31. Araya N, Takahashi K, Sato T, Nakamura T, Sawa C, et al. (2011) Fucoidan therapy decreases the proviral load in patients with human T-lymphotropic virus type-1-associated neurological disease. Antivir Ther 16: 89–98.
32. Olindo S, Lézin A, Cabre P, Merle H, Saint-Vil M, et al. (2005) HTLV-1 proviral load in peripheral blood mononuclear cells quantified in 100 HAM/TSP patients: a marker of disease progression. J Neurol Sci 237: 53–59.
33. Müller M, Carter S, Hofer MJ, Campbell IL (2010) Review: The chemokine receptor CXCR3 and its ligands CXCL9, CXCL10 and CXCL11 in neuroimmunity-a tale of conflict and conundrum. Neuropathol Appl Neurobiol 36: 368–387.
34. Murr C, Widner B, Wirleitner B, Fuchs D (2002) Neopterin as a marker for immune system activation. Curr Drug Metab 3: 175–187.
35. Ijichi S, Izumo S, Eiraku N, Machigashira K, Kubota R, et al. (1993) An autoaggressive process against bystander tissues in HTLV-I-infected individuals: a possible pathomechanism of HAM/TSP. Med Hypotheses 41: 542–547.
36. Bangham CR, Osame M (2005) Cellular immune response to HTLV-1. Oncogene 24: 6035–6046.
37. Matsuura E, Yamano Y, Jacobson S (2010) Neuroimmunity of HTLV-I Infection. J Neuroimmune Pharmacol 5: 310–325.
38. Lezin A, Olindo S, Oliere S, Varrin-Doyer M, Marlin R, et al. (2005) Human T lymphotropic virus type I (HTLV-I) proviral load in cerebrospinal fluid: a new criterion for the diagnosis of HTLV-I-associated myelopathy/tropical spastic paraparesis? J Infect Dis 191: 1830–1834.
39. Puccioni-Sohler M, Yamano Y, Rios M, Carvalho SM, Vasconcelos CC, et al. (2007) Differentiation of HAM/TSP from patients with multiple sclerosis infected with HTLV-I. Neurology 68: 206–213.
40. Takenouchi N, Yamano Y, Usuku K, Osame M, Izumo S (2003) Usefulness of proviral load measurement for monitoring of disease activity in individual patients with human T-lymphotropic virus type I-associated myelopathy/tropical spastic paraparesis. J Neurovirol 9: 29–35.
41. Hayashi D, Kubota R, Takenouchi N, Nakamura T, Umehara F, et al. (2008) Accumulation of human T-lymphotropic virus type I (HTLV-I)-infected cells in the cerebrospinal fluid during the exacerbation of HTLV-I-associated myelopathy. J Neurovirol 14: 459–463.
42. Milagres AC, Jorge ML, Marchiori PE, Segurado AA (2002) Human T cell lymphotropic virus type 1-associated myelopathy in São Paulo, Brazil. Epidemiologic and clinical features of a university hospital cohort. Neuroepidemiology 21: 153–158.
43. Araya N, Sato T, Yagishita N, Ando H, Utsunomiya A, et al. (2011) Human T-lymphotropic virus type 1 (HTLV-1) and regulatory T cells in HTLV-1-associated neuroinflammatory disease. Viruses 3: 1532–1548.
44. Yamano Y, Araya N, Sato T, Utsunomiya A, Azakami K, et al. (2009) Abnormally high levels of virus-infected IFN-gamma+ CCR4+ CD4+ CD25+ T cells in a retrovirus-associated neuroinflammatory disorder. PLoS One 4: e6517.

Regular Article

LYMPHOID NEOPLASIA

Preapoptotic protease calpain-2 is frequently suppressed in adult T-cell leukemia

Makoto Ishihara,[1] Natsumi Araya,[2] Tomoo Sato,[2] Ayako Tatsuguchi,[1] Naomi Saichi,[1] Atae Utsunomiya,[3] Yusuke Nakamura,[4] Hidewaki Nakagawa,[1] Yoshihisa Yamano,[2] and Koji Ueda[1]

[1]Laboratory for Biomarker Development, Center of Genomic Medicine, RIKEN, Tokyo, Japan; [2]Department of Molecular Medical Science, Institute of Medical Science, St. Marianna University School of Medicine, Kawasaki, Japan; [3]Department of Hematology, Imamura Bun-in Hospital, Kagoshima, Japan; and [4]Section of Hematology/Oncology, Department of Medicine Faculty, The University of Chicago, Chicago, IL

Key Points

- Proteome-wide analysis of HTLV-1–infected T cells identified 17 biomarker proteins for the diagnosis of ATL or HAM/TSP patients.

Adult T-cell leukemia (ATL) is one of the most aggressive hematologic malignancies caused by human T-lymphotropic virus type 1 (HTLV-1) infection. The prognosis of ATL is extremely poor; however, effective strategies for diagnosis and treatment have not been established. To identify novel therapeutic targets and diagnostic markers for ATL, we employed focused proteomic profiling of the $CD4^+CD25^+CCR4^+$ T-cell subpopulation in which HTLV-1–infected cells were enriched. Comprehensive quantification of 14 064 peptides and subsequent 2-step statistical analysis using 29 cases (6 uninfected controls, 5 asymptomatic carriers, 9 HTLV-1–associated myelopathy/tropical spastic paraparesis patients, 9 ATL patients) identified 91 peptide determinants that statistically classified 4 clinical groups with an accuracy rate of 92.2% by cross-validation test. Among the identified 17 classifier proteins, α-II spectrin was drastically accumulated in infected T cells derived from ATL patients, whereas its digestive protease calpain-2 (CAN2) was significantly downregulated. Further cell cycle analysis and cell growth assay revealed that rescue of CAN2 activity by overexpressing constitutively active CAN2 (Δ_{19}CAN2) could induce remarkable cell death on ATL cells accompanied by reduction of α-II spectrin. These results support that proteomic profiling of HTLV-1–infected T cells could provide potential diagnostic biomarkers and an attractive resource of therapeutic targets for ATL. (*Blood*. 2013;121(21):4340-4347)

Introduction

Human T-lymphotropic virus type 1 (HTLV-1) is a human retrovirus that is the pathogenic agent of HTLV-1–associated diseases, such as adult T-cell leukemia (ATL) and HTLV-1–associated myelopathy/tropical spastic paraparesis (HAM/TSP). Recent epidemiological studies revealed that HTLV-1 is endemic mainly in Japan, the Caribbean basin, Iran, Africa, South America, and the Melanesian islands.[1] Other estimates have shown that 20 million to 30 million people worldwide are infected with HTLV-1.[2] The infection is followed by a prolonged asymptomatic phase of 20 to 30 years, and 2% to 5% of the infected individuals develop ATL during their lifetime.[3] ATL is one of the most aggressive hematologic malignancies characterized by increased numbers of lymphocytes with multilobulated nuclei, so-called flower cells, in blood circulation. The prognosis is severe with the median overall survival period and 5-year survival rate of ATL patients of 7 months and 20%, respectively.[4] Recently, humanized anti-CCR4 (KW-0761) therapeutic antibody achieved a great improvement in ATL treatment in a phase 3 study. However, the disease control rate was restricted to 50%, and long-term prognosis has yet to be known.[5] For future improvements in the management of ATL, novel biomarkers for early diagnosis are urgently needed for early therapeutic intervention.

To date, comprehensive genomic or proteomic studies using $CD4^+$ T cells have been performed for this purpose,[6-9] but reproducibility and reliability of quantification results in the discovery phase were uncertain due to the diverse individual variety of HTLV-1–infected cell contents in $CD4^+$ T cells. To overcome the etiologic variety of samples, we focused on the $CD4^+CD25^+CCR4^+$ T-cell subpopulation since Yamano et al[10] recently revealed that HTLV-1 preferentially infected $CD4^+CD25^+CCR4^+$ T cells in both ATL and HAM/TSP patients. By targeting $CD4^+CD25^+CCR4^+$ T cells, we here provide the first quantitative proteome map illustrating molecular disorders in pathogenic human T cells directly associated with the onset or progression of ATL. The comprehensive and comparative interpretation of total proteome in infected cells, especially between asymptomatic HTLV-1 carriers and ATL patients, could immediately lead to specific candidates for biomarkers and drugs.

Another challenge to emphasize in this study is our recently established proteomic profiling technologies. It is indisputable that the greater the number of clinical samples analyzed, the more confidently statistical analysis can be undertaken in order to identify diagnostic markers and druggable targets. Despite this fact, previous proteomics reports could not provide high-throughput quantitative methodologies that were sufficient for dealing with even more than 10 clinical samples, excepting a study utilizing a surface enhanced laser desorption/ionization time of flight mass spectrometer. Although the surface enhanced laser desorption/ionization time of flight method drastically improved the performance in both quantification and throughput, allowing relative quantification

Submitted August 1, 2012; accepted March 25, 2013. Prepublished online as *Blood* First Edition paper, March 28, 2013; DOI 10.1182/blood-2012-08-446922.

The online version of this article contains a data supplement.

The publication costs of this article were defrayed in part by page charge payment. Therefore, and solely to indicate this fact, this article is hereby marked "advertisement" in accordance with 18 USC section 1734.

analysis for 96 samples in several hours, at most only 250 unidentified protein peaks were detectable. In the present study, we integrated the proteomics server for the huge data set "Expressionist" (Genedata A.G., Basel, Switzerland) with high-end mass spectrometers to maximize the quality and quantity of protein catalogs transferred from mass spectrometers. We first describe the discovery phase providing a panel of novel diagnostic molecules from quantification of 14 064 peptides and identification of 4763 proteins. As the functional validation phase, we further examined the physiological potential of an identified diagnostic marker candidate, calpain-2 (CAN2), particularly concerning the association of its activity with survival or progression of ATL cells.

Materials and methods

PBMCs and cell lines

Peripheral blood mononuclear cells (PBMCs) from 6 normal donors, 5 asymptomatic carriers, and 9 HAM/TSP patients used in the screening analysis were collected in the St. Marianna University School of Medicine. Those from 9 ATL patients were collected in the Imamura Bun-in Hospital. PBMCs from 4 ATL patients used for the validation experiments were provided by the Joint Study on Predisposing Factors of ATL Development. The others from 4 HAM/TSP patients were collected in the St. Marianna University School of Medicine. The use of these human specimens in this study was approved by individual institutional ethical committees: the Ethical Committee of Yokohama Institute, RIKEN (approval code Yokohama H22-3); the Ethical Committee of St. Marianna University School of Medicine; the Institutional Review Board of Imamura Bun-in Hospital; and the Ethical Committee of the University of Tokyo (approval code 10-50). This study was conducted in accordance with the Declaration of Helsinki.

SO-4, KOB, and KK1 cells were kindly provided by Dr Yasuaki Yamada, cultured in RPMI 1640 supplemented with 10% fetal bovine serum (Cell Culture Bioscience, Tokyo, Japan), 100 kU/L interleukin 2 (Cell Science & Technology Institute Inc., Tokyo, Japan), and 1 × antibiotic-antimycotic solution (Sigma-Aldrich, MO). Jurkat, SUP-T1, CCRF-CEM, and MOLT-3 cells were cultured in RPMI 1640 supplemented with 10% fetal bovine serum and 1 × antibiotic-antimycotic solution. All cell lines were grown at 37°C in 5% CO_2. $CD3^+CD4^+CD25^+CCR4^+$ T cells were isolated with anti-CD3-FITC (eBioscience, San Diego, CA), anti-CCR4-PE (Becton Dickinson, CA), anti-CD4-Cy7 (eBioscience), and anti-CD25-APC (eBioscience) on a Cell Sorter JSAN (Bay Bioscience, Hyogo, Japan).

Sample preparation for mass spectrometric analysis

The $CD4^+CD25^+CCR4^+$ T cells were washed with phosphate-buffered saline 3 times and lysed in denaturation buffer (8 M urea in 50 mM ammonium bicarbonate). After sonication, reduction with 5 mM tris(2-carboxyethyl) phosphine (Sigma-Aldrich) at 37°C for 30 minutes, and alkylation with 25 mM iodacetamide (Sigma-Aldrich) at room temperature for 45 minutes, lysates were digested with Trypsin GOLD (Promega, WI) with protein/enzyme ratio of 25:1 at 37°C for 12 hours. The digested peptides were desalted with Oasis HLB μElution plate (Waters, MA). The collected samples were dried up with a Vacuum Spin Drier (TAITEC Co. Ltd., Saitama, Japan) and subjected to mass spectrometric analyses.

Liquid chromatography tandem mass spectrometry (LC/MS/MS)

The digested peptides were separated on a 0.1 × 200 mm homemade C_{18} column using a 2-step linear gradient, 2% to 35% acetonitrile for 95 minutes and 35% to 95% acetonitrile for 15 minutes in 0.1% formic acid with a flow rate of 200 nL/min. The eluting peptides were analyzed with a QSTAR-Elite mass spectrometer (AB Sciex, CA) in the smart information-dependent acquisition mode of Analyst QS software 2.0 (AB Sciex). The other parameters on QSTAR-Elite were shown as follows: DP = 60, FP = 265, DP2 = 15, CAD = 5, IRD = 6, IRW = 5, curtain gas = 20, and ion spray voltage = 2000 V.

Two-dimensional (2D) LC/MS/MS

Tryptic digests of $CD4^+CD25^+CCR4^+$ T cells were dissolved in 10 mM ammonium formate in 25% acetonitrile and fractionated by a 0.2 × 250 mm monolith strong cation exchange column (GL Science, Tokyo, Japan). Peptides were eluted with an ammonium formate gradient from 10 mM to 1 M in curve = 3 mode for 70 minutes using a Prominence high-performance liquid chromatography (HPLC) system (Shimadzu Corporation, Kyoto, Japan). The eluate was fractionated into 20 fractions and analyzed individually by LTQ-Orbitrap-Velos mass spectrometer (Thermo Scientific, Bremen, Germany) accompanied with the Ultimate 3000 nano-HPLC system. The fractionated peptide samples were separated with the same gradient used in the QSTAR-Elite system described previously and analyzed by LTQ-Orbitrap-Velos acquiring a full MS scan on Fourier-transition mode with MS resolution = 60 000 and simultaneously MS/MS scans for the 20 most intense precursor ions in each MS spectrum on ion-trap mode with regular resolution. Other important parameters for LTQ-Orbitrap-Velos were as follows: capillary temp = 250, source voltage = 2 kV, MS scan range = mass-to-charge ratio (m/z) 400 to 1600, acquire data dependent CID MS/MS for top-20 intense precursors, and dynamic exclusion enabled during 30 seconds. For protein identification, all MS/MS spectra were searched against SwissProt database version 2012_06 (20 232 human protein sequences) using SEQUEST algorithm on ProteomeDiscoverer 1.3 software (Thermo Scientific) with the following parameters: MS tolerance = 3 ppm, MS/MS tolerance = 0.8 Da, maximum missed cleavages = 2, enzyme = trypsin, taxonomy = *Homo sapiens*, fixed modification = carbamidomethylation on cysteine, and variable modification = oxidation on methionine. We accepted the protein identification satisfying the false discovery rate <1% by Percolator false discovery rate estimation algorithm on ProteomeDiscoverer.

Label-free quantification analysis

The LC/MS/MS raw data were imported into the Expressionist RefinerMS module and subjected to the following data processing and relative quantification steps. The total work flow on the RefinerMS module is shown in supplemental Figure 1 (see the *Blood* Web site). The LC/MS/MS raw data set from 29 clinical samples was displayed in 2D planes (m/z vs retention time [RT]). The chromatogram grid was applied to all planes: scan counts = 10, polynom order = 3, and RT smoothing = 0. The planes were simplified by subtracting background noises using chromatogram chemical noise subtraction: RT window = 50 scans, quantile subtraction = 50%, and RT smoothing = 3 scans. After the noise subtraction, data points with intensity <10 were clipped to zero. The RT variety among 29 planes was adjusted by chromatogram RT alignment: RT transformation window = 0.2 minutes, RT search interval = 5 minutes, m/z window = 0.1 Da, and gap penalty = 1. Peaks were detected by chromatogram summed peak detection: summation window = 5 scans, overlap = 50, minimum peak size = 4 scans, maximum merge distance = 10 points, peak RT splitting = true, intensity profiling = max, gap/peak ratio = 1%, refinement threshold = 5, consistency threshold = 0.8, and signal/noise threshold = 1. The detected peaks were grouped into isotopic clusters derived from each molecule using 2-step chromatogram isotopic peak clustering. The first parameters were as follows: minimum charge = 1, maximum charge = 10, maximum missing peaks = 0, first allowed gap position = 3, RT window = 0.1 minute, m/z tolerance = 0.05 Da, isotope shape tolerance = 10, and minimum cluster size ration = 1.2. The second parameters were as follows: minimum charge = 1, maximum charge = 10, maximum missing peaks = 0, first allowed gap position = 3, RT window = 0.1 minute, m/z tolerance = 0.05 Da, and minimum cluster size ration = 0.6.

Expression vectors and siRNA

For the Δ_{19}CAN2 construct, the *CAPN2* fragment was amplified with primers 5′-CATGTCGACTCCCACGAGAGGGCCATCAAGT-3′ and 5′-CATTCTAGATCAAAGTACTGAGAAACAGAGCC-3′ from pBlueBacIII *CAPN2* and cloned into pEFBOS-Myc. Prior to the overexpression experiments, we confirmed that the sequence of the inserted *CAPN2* fragment was identical to the Mammalian Gene Collection sequence (accession number

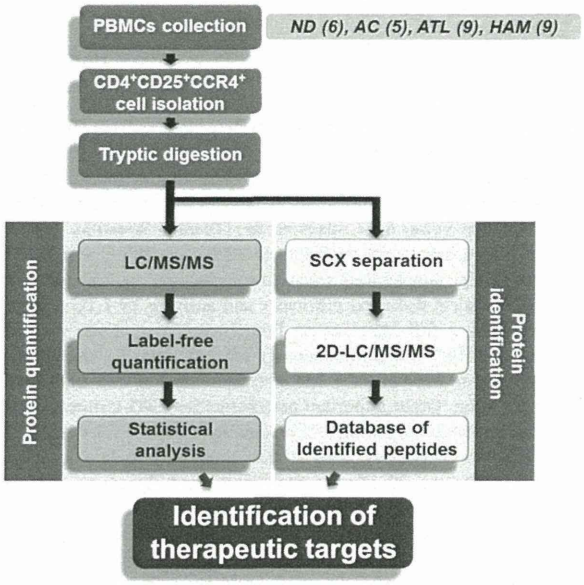

Figure 1. Schematic overview of proteomic profiling for $CD4^+CD25^+CCR4^+$ cells. PBMCs were collected from 6 normal donors, 5 asymptomatic carriers, 9 ATL patients, and 9 HAM/TSP patients, followed by isolation of the $CD4^+CD25^+CCR4^+$ subset using the cell-sorting system. The statistical candidate selection steps, including LC/MS/MS data processing, label-free quantification, and statistical analysis, were performed on the Expressionist proteome server. The protein identification database was separately established based on 2D LC/MS/MS analysis. ND, normal donors; AC, asymptomatic carriers.

BC021303). The 5-μg vector DNA was transfected to 1×10^6 cells. The small interfering RNAs (siRNAs) against *SPTAN1*, *PTMS*, *HSPE1*, and SHMT2 and siRNA universal negative control were purchased from Sigma-Aldrich. The 500-pmol siRNA oligo was transfected into 1×10^6 cells. The vectors and siRNAs were transfected into all cell lines except CCRF-CEM by Amaxa Nucleoportator transfection Kit V (Lonza, Cologne, Germany) and CCRF-CEM by Kit C (Lonza).

Cell cycle analysis and proliferation assay

For the cell cycle analysis, 1×10^5 to 2×10^5 cells were washed and agitated in 0.1% Triton-X (Sigma-Aldrich) with 100 ng/mL of ribonuclease (Sigma-Aldrich). Following addition of 1 μg/mL propidium iodide, the flow cytometric analysis was performed on FACScalibur (Becton Dickinson). The data analysis was performed using FlowJo software (Tree Star Inc., OR). Doublet events were eliminated from analyses by proper gating on FL2-W/FL2-A primary plots before histogram analysis of DNA content. Cell proliferation was estimated by measuring cell metabolic activity using Cell Counting Kit-8 (Dojindo, Kumamoto, Japan) following the manufacturer's recommendation.

Western blotting

Cells were lysed in lysis buffer [1% NP-40, 2 mM EGTA, 2 mM $MgCl_2$, 150 mM NaCl, 20 mM tris(hydroxymethyl)aminomethane–HCl (pH 7.5), 10% glycerol, containing the protease inhibitor cocktail Complete (Roche, IN)] and subjected to sodium dodecyl sulfate–polyacrylamide gel electrophoresis and transferred onto PVDF membranes. Following blocking with 4% Block Ace (Yukijirushi Nyugyo Inc., Tokyo, Japan), membranes were incubated with anti-myc (9E10; Sigma-Aldrich) or anti–α-II spectrin (Abcam, Cambridge, UK) antibodies. Membranes were then incubated with horseradish peroxidase–conjugated anti-mouse IgG (GE Healthcare, NJ) or anti-rabbit IgG (GE Healthcare), respectively, and visualized with Western Lightning kit (Perkin Elmer, MA).

Multiple reaction monitoring (MRM)

$CD4^+$ T cells were isolated from PBMCs using flow cytometry. The tryptic digests of the isolated cells were analyzed by 4000 Q-TRAP mass spectrometer (AB Sciex) accompanied with Ultimate 3000 nano-HPLC system. The LC gradient was as follows: 2% to 30% acetonitrile for 10 minutes and 30% to 95% acetonitrile for 5 minutes in 0.1% formic acid with a flow rate of 300 nL/min. The MRM transitions monitored were m/z 409.7/375.2 for α-II spectrin (SPTA2); m/z 538.3/889.5 for parathymosin (PTMS); m/z 507.3/147.1 for heat shock 10-kDa protein, mitochondrial (CH10); m/z 490.3/147.1 for serine hydroxymethyltransferase, mitochondrial (GLYM); and m/z 581.3/919.5 for β-actin, respectively. Individual peak areas were normalized by the peak area of β-actin. Data acquisition was performed with ion spray voltage = 2300 V, curtain gas = 10 psi, nebulizer gas = 10 psi, and an interface heating temperature = 150°C. The parameters were set as follows: declustering potential = 60, entrance potential = 10, collision cell exit potential = 10, and dwell time for each transition = 10 seconds. Collision energy was optimized to achieve maximum intensity for each MRM transition as follows: 34.03 V for m/z 409.7/175.1, 24.68 eV for m/z 538.3/889.5, 23.32 eV for m/z 507.3/147.1, 37.57 eV for m/z 490.3/147.1, and 31.58 eV for m/z 581.3/919.5.

Results

Quantitative proteome profiling of $CD4^+CD25^+CCR4^+$ T cells

A schematic overview of the screening approach is shown in Figure 1. To identify diagnostic markers expressed in HTLV-1–infected T cells, a $CD4^+CD25^+CCR4^+$ subset of PBMCs from 6 uninfected volunteers, 5 asymptomatic carriers, 9 HAM/TSP patients, and 9 ATL patients was isolated by flow cytometry (Figure 2). The averaged proportion of $CD4^+CD25^+CCR4^+$ cells in $CD4^+$ T cells from 4 clinical groups was 6.48 ± 2.46%, 13.17 ± 13.06%, 20.55 ± 10.73%, and 55.83 ± 22.40%, respectively, indicating that the occupancy of viral reservoir cells varied drastically among both pathological groups and even individuals within a group. Enrichment of the infected cells was confirmed by viral load measurement of the used samples (supplemental Figure 2). As reported previously,[10] the viral load of $CD4^+CD25^+CCR4^+$ cells (37.91 copies/100 cells on average) was ~10 times higher than that of $CD4^+CD25^-CCR4^-$ cells (4.12 copies/100 cells on average), indicating that the former cells were evidently the HTLV-1–enriched fraction. This fact strongly supports the importance of

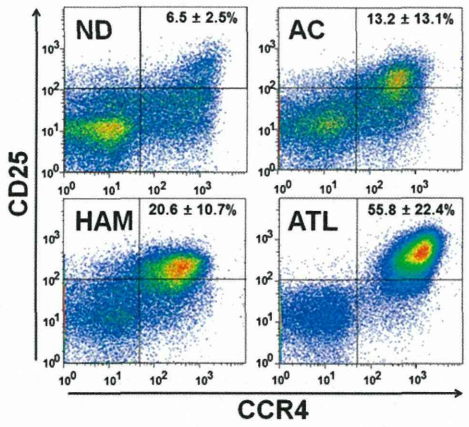

Figure 2. Representative sorting results of $CD4^+CD25^+CCR4^+$ cells. After labeling with anti-CD3-FITC, anti-CD4-Cy7, anti-CD25-APC, and anti-CCR4-PE, the $CD3^+CD4^+CD25^+CCR4^+$ fraction was isolated. The averaged content ± standard deviation (%) of $CD25^+CCR4^+$ cells out of $CD3^+CD4^+$ cells was calculated for each clinical group and is displayed in the upper right section of the panels.

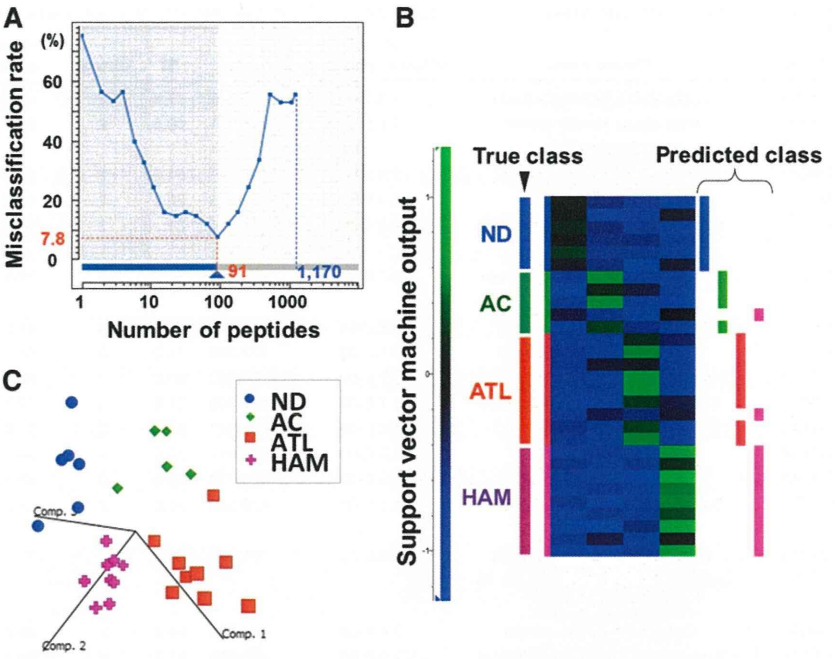

Figure 3. Statistical extraction of candidate therapeutic targets. The 14 064 nonredundant peptides detected were subjected to a 4-group Kruskal-Wallis test (ND, AC, ATL, and HAM), resulting in identification of 1170 first candidates ($P < .01$). ND, normal donors; AC, asymptomatic carriers. (A) Next, the Expressionist ranking method further narrowed down the candidates to 91 peptides based on SVM-REF so that the misclassification rate in the cross-validation test became minimum, 7.8%. (B) The predicted classification result by leave-one-out cross-validation test. The 27 out of 29 cases were successfully classified into the true classes. (C) The three-dimensional plot shows the additional assessment for the classification power of 91 classifiers by principal component analysis. Comp. 1 to 3 indicate principal components 1 to 3.

enriching pathogenic cells for rigorous quantitative biomarker discovery.

An accurately adjusted number of $CD4^+CD25^+CCR4^+$ cells from 29 cases were digested with trypsin and subjected to LC/MS/MS analysis individually. Because recent mass spectrometers often deal with data on the order of hundreds of megabytes per sample, it has been considered almost impossible to calculate a data set larger than a gigabyte from large-scale clinical samples on desktop computers. Hence, we constructed a proteomics server equipped with a 12-core central processing unit, 36 SAS hard disks, and 192-GB physical memories driving the Expressionist, which was designed to combine the database module, the data processing module, and the statistical analysis module into a single integrative platform for genomics, proteomics, and metabolomics. The detailed work flow for data processing and quantification for 29 LC/MS/MS raw data was described in the "Materials and methods" and is illustrated in supplemental Figure 1. Finally, 68 454 nonredundant peaks were detected and grouped into 37 143 isotopic clusters, or molecules. As tryptic peptides should appear as multivalent ions in electrospray ionization mass spectra, 23 079 singly charged ions were removed, resulting in utilization of 14 064 peptide signals for further statistical selection of diagnostic markers.

Statistical identification of candidate diagnostic markers for ATL

A stepwise statistical extraction was employed for the effective identification of proteins, which demonstrated specific up- or downregulation in the ATL group. In the first stage, a 4-group Kruskal-Wallis test was performed to roughly extract the candidates showing a significantly distinct expression level among 4 clinical groups. Here we set the cutoff line at $P < .01$ and obtained 1170 first candidate peptides simply because the isolated peptide set using this criterion showed the best performance in the following prediction model.

Next, we selected the final candidates by the support vector machine–recursive feature elimination algorithm in the Expressionist Analyst module. Support vector machine–recursive feature elimination is a candidate elimination method based on SVM, which enabled us to improve the classification outputs by selecting the best-performing peptide set among initially provided candidates.[11] As a result, a combination of 91 peptides showed the lowest misclassification rate (7.78%) in a leave-one-out cross-validation test (Figure 3A-B). To evaluate the classification efficiency of 91 selected candidates, the principal component analysis was performed. Figure 3C shows the three-dimensional plot of 29 clinical samples based on the 3 best-explainable components, which illustrated statistically clear segregation among the 4 clinical groups. These assessments indicated that the 91 peptides should be a sufficient set of classifiers that closely associated with the pathological characteristics of the 4 clinical groups.

Based on an independently constructed 6279-protein identification database for $CD4^+CD25^+CCR4^+$ cells using 2D LC/MS/MS (see details in "Materials and methods"), 19 peptides among the 91 candidate peptides were successfully assigned to 17 proteins listed in Table 1. The mass spectrometric quantification profiles for the 19 peptides are also shown in Figure 4 (box plots).

Recovering CAN2 activity induced cell death in ATL cells

Our diagnostic marker discovery for ATL identified an enzyme-substrate pair, CAN2 and SPTA2, which demonstrated significantly aberrant expression level in ATL patients (Figure 4). Interestingly, the intensities of the 2 proteins in 27 screening cases (without 2 statistical outliers in Figure 4) showed a clearly inverse correlation ($R^2 = 0.395$, Figure 5A). To examine whether CAN2 downregulation and/or SPTA2 upregulation might be essential for the growth of ATL cells, the enzymatic activity of CAN2 was rescued by overexpressing the constitutively active form of CAN2 (Δ_{19}CAN2) in 3 ATL cell lines, SO-4, KOB, and KK1. After 36 hours of transfection, significant inhibition of cell proliferation (Figure 5B) and induction of sub-G1 transition was observed by activation of CAN2 in 3 ATL cells, but not in 4 non-ATL leukemia cell lines (Figure 5C). Furthermore, overexpression of Δ_{19}CAN2 drastically attenuated the expression level of SPTA2 in the ATL cell

Table 1. List of 17 protein classifiers for categorization of normal donors, asymptomatic carriers, HAM/TSP, and ATL

Accession	Protein name	*P* value (Kruskal-Wallis test)	m/z	RT	Charge	Peptide score	Identity or homology threshold	Sequence
LPPL	Eosinophil lysophospholipase	2.3.E-03	409.722	47.4	2	36.3	27	MVQVWR
CH10	Heat shock 10-kDa protein, mitochondrial	2.5.E-03	430.721	40.6	2	26.2	21	GGIMLPEK
PRG2	Bone marrow proteoglycan	2.4.E-03	528.271	64.6	2	31.6	28	RLPFICSY
MOES	Moesin	8.1.E-04	532.253	26.8	2	46.2	29	EKEELMER
MNDA	Myeloid cell nuclear differentiation antigen	9.4.E-03	647.863	69.1	2	67.3	24	SLLAYDLGLTTK
GLYM	Serine hydroxymethyltransferase, mitochondrial	8.7.E-04	408.551	21.6	3	31.1	18	HADIVTTTTHK
PTMS	Parathymosin	9.7.E-04	453.875	17.8	3	41.2	25	AAEEEDEADPKR
TPIS	Triosephosphate isomerase	9.1.E-03	472.266	71.0	3	54.0	28	QSLGELIGTLNAAK
HSP71	Heat shock 70-kDa protein 1A/1B	9.7.E-03	563.307	65.5	3	93.8	21	IINEPTAAAIAYGLDR
CD6	T-cell differentiation antigen CD6	7.7.E-03	592.306	37.8	3	62.7	22	VLCQSLGCGTAVERPK
ANXA1	Annexin A1	4.4.E-04	612.347	61.5	3	57.0	17	RKGTDVNVFNTILTTR
ANXA6	Annexin A6	2.3.E-03	669.017	70.9	3	54.7	16	AMEGAGTDEKALIEILATR
SPTA2	Spectrin α chain, brain	5.4.E-03	409.718	28.8	2	42.7	30	EAGSVSLR
GLYM	Serine hydroxymethyltransferase, mitochondrial	1.1.E-03	428.240	57.0	2	42.8	27	SGLIFYR
DRB1s	HLA class II histocompatibility antigen, DRB1-1, 4, 10, 11, 13, 15, 16 β chain	1.0.E-02	478.216	25.8	2	55.9	25	AAVDTYCR
CAN2	Calpain-2 catalytic subunit	2.4.E-03	483.253	54.0	2	66.6	29	SDTFINLR
STAT1	Signal transducer and activator of transcription 1-α/β	7.3.E-03	486.290	21.7	2	39.1	29	KILENAQR
PRG2	Bone marrow proteoglycan	9.4.E-04	497.742	49.2	2	31.6	27	FQWVDGSR
CXCL7	Platelet basic protein	1.3.E-03	528.761	43.1	2	51.7	28	ICLDPDAPR

line SO-4 (Figure 5D), but not in the non-ATL leukemia cell line Jurkat (Figure 5E). On the other hand, an additional cell proliferation assay using siRNA against *SPTAN1* revealed that reduction of SPTA2 was not sufficient for the induction of cell death for ATL cells (supplemental Figures 3 and 4).

In addition, 3 proteins (PTMS, CH10, and GLYM) were also found to be upregulated in ATL cells. To address the roles of these proteins, a cell proliferation assay was conducted using 3 ATL cell lines treated with siRNAs against *PTMS*, *HSPE1* (gene symbol of CH10), or *SHMT2* (gene symbol of GLYM) (supplemental Figure 4). As a result, suppression of the *SHMT2* gene induced significant growth inhibition for all 3 ATL cell lines. Although si*HSPE1*-treated KOB cells showed a statistically significant decrease in cell growth rate, si*HSPE1* and si*PTMS* had only partial

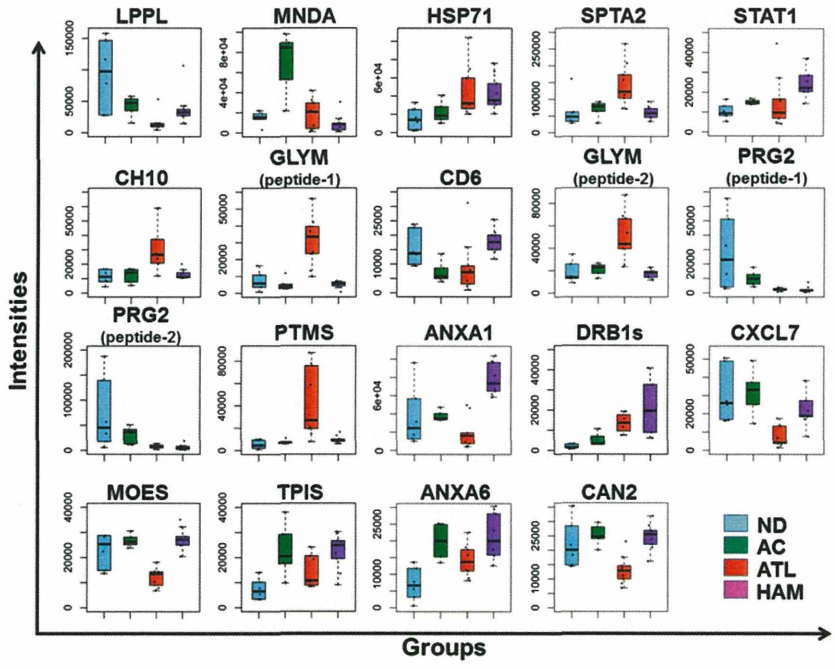

Figure 4. Summary of quantitative features for the 17 protein classifiers identified. The 19 box plots (see Table 1 for protein names) show the results of mass spectrometric quantification and protein identification. We finally identified 19 peptides out of 91 candidates in Figure 3, which were assigned to 17 proteins. Proteins identified from 2 distinct peptides were shown as GLYM (peptides 1 and 2) or PRG2 (peptides 1 and 2). The y-axis indicates normalized relative intensity of peptides in mass spectrometric data. ND, normal donors; AC, asymptomatic carriers.

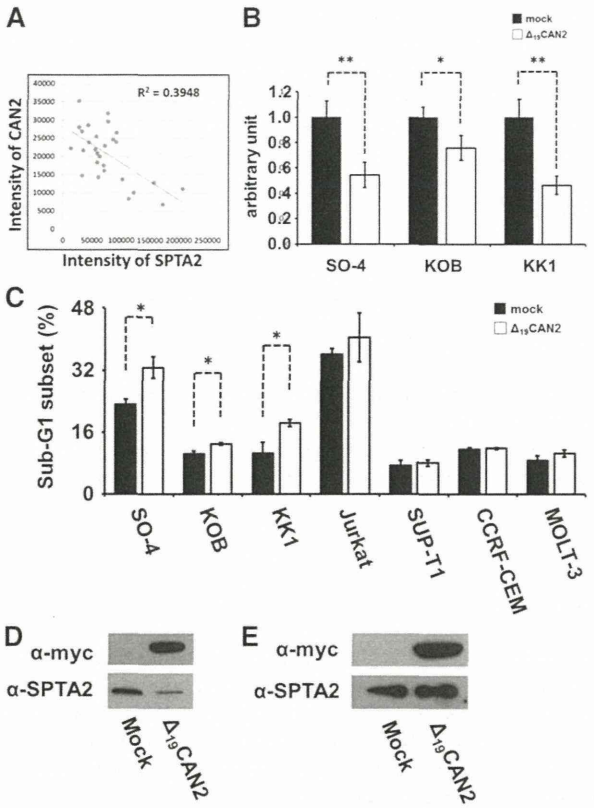

Figure 5. Rescue of CAN2 activity induced cell death in ATL cells. (A) Correlation between CAN2 and SPTA2 expression level in 27 cases. (B) Cell proliferation was measured by MTT assay on SO-4, KOB, and KK1 cells 36 hours after transfection of mock vector or Δ_{19}CAN2. $^{*}P < .05$; $^{**}P < .01$ by Student *t* test. (C) Overexpression of Δ_{19}CAN2 significantly accelerated cell death in 3 ATL (SO-4, KOB, and KK1) and 4 non-ATL (Jurkat, SUP-T1, CCRF-CEM, and MOLT-3) cell lines. $^{**}P < .05$ by Student *t* test. The drastic attenuation of SPTA2 expression was observed after transfection of Δ_{19}CAN2 in SO-4 cells (D), but not in Jurkat cells (E). The immunoblot of anti-myc tag confirmed the expression of exogenous Δ_{19}CAN2.

or no effects on proliferation of ATL cell lines. To further confirm whether the overexpression of SPTA2, PTMS, CH10, or GLYM protein would be an ATL-specific molecular signature, the expression levels of these proteins in 8 clinical samples were evaluated by the mass spectrometric quantification technology MRM (supplemental Figures 5 and 6). Expression of SPTA2, GLYM, and CH10 in cells derived from ATL patients was significantly higher than that in cells derived from HAM/TSP patients. The level of PTMS also showed a clearly increasing tendency in the ATL patient group. Taken together, these results suggested that the deprivation of CAN2 activity and upregulation of GLYM in HTLV-1–infected T cells might have a key role at the onset or progression of ATL.

Discussion

In the past decade, proteomics technologies have developed dramatically for the purpose of obtaining more and more comprehensive and sensitive proteome maps in cells or clinical specimens. The performance of mass spectrometers in particular has exhibited remarkable progress; however, as for sensitivity and throughput, it has still been difficult to identify biomarkers from crude samples including body fluids or total cell lysate. A major reason could be that the range of protein concentration in the analyte is indeed much larger than the dynamic range of recent mass spectrometers.[12] The other essential factor to be improved for clinical proteomics is the capacity of the bioinformatics platform to allow analysis of a sufficient number of clinical samples in order to statistically overcome the significant individual variability.[13]

Concerning the first issue, we previously developed and applied various focused proteomic applications targeting molecular biochemical features including glycan structure biomarkers[14-16] and low-molecular-weight peptide biomarkers.[17] The preenrichment of subproteome fractions effectively reduces the complexity of crude samples and allowed us to identify potential serum cancer biomarkers successfully. Through our previous knowledge, we provide an approach for investigating infectious diseases by employing virus-infected cell-focused proteomics. In addition to HTLV-1, for instance, isolation of HIV-infected cells is highly desired because the frequency of these cells in AIDS patients' PBMCs is ~1 out of 10^4 to 10^5 cells.[18] Actually, we successfully demonstrated the effect of HTLV-1–infected cell isolation on the elimination of individual variability (Figure 2, supplemental Figure 2) and reliable identification of disease state–associated proteins (Figures 4 and 5). We further showed the potential of the next-generation bioinformatics platform Expressionist to remove the constraint on the capacity of data size acquired from high-end mass spectrometers. Expressionist covered whole discovery steps from processing of raw mass spectrometer data to statistical analyses (Figures 1 and 3, and supplemental Figure 1) and, importantly, could perform quantification analysis using a basically unlimited number of clinical samples. Hence, in parallel with the development of mass spectrometers, high-specification and inexpensive OMICS server systems are necessary for future diagnostic marker and therapeutic target discoveries using hundreds or thousands of clinical specimens.

In this study, we focused on the $CD4^+CD25^+CCR4^+$ T-cell subpopulation in which T helper 2, T helper 17, and regulatory T (Treg) cells were mainly involved.[10] The purpose for which we used this subset was to technically enrich the preferential viral reservoir cells and to strengthen reliability of screening results. However, investigating proteome behaviors of these subtypes in HTLV-1–associated diseases is also important physiologically because it has been frequently reported that deregulated Treg plays significant roles in pathogenesis of ATL and HAM/TSP. Indeed, aberrant proliferation of Treg cells is considered the main cause of immunodeficiency in ATL patients because of their innate immunosuppressive functions,[19] whereas abnormal production of interferon γ from infected Treg cells might induce chronic spinal inflammation in HAM/TSP patients.[20] Given the list of our 17 classifier proteins, activation of signal transducer and activator of transcription 1-α/β is the well-known key factor for HAM/TSP,[21] whereas upregulation of heat shock 70-kDa protein 1A/1B, CH10, and PTMS were reported in many other types of tumors.[22-24] The association of these 4 proteins with the etiology of HAM/TSP and ATL would be evident according to the previous work, supporting that our other candidates might similarly have a direct impact on the transformation of Treg cells after infection of HTLV-1. Particularly, the specific upregulation of GLYM in ATL cells represents the first evidence that excessive folate metabolism might be essential for the progression or survival of ATL cells because GLYM is a fundamental enzyme catalyzing the supply of glycine accompanying the conversion of tetrahydrofolate to 5,10-methylenetetrahydrofolate.[25] Indeed, the suppression of GLYM expression, which was confirmed to be upregulated in ATL patients, resulted in significant reduction of cell growth. This observation suggests that diminishing GLYM

expression or enzyme activity could be a promising strategy for molecular-targeting treatment of ATL. Together with the downregulation of CAN2 in the ATL cells shown in Figure 5, the proteins listed in Table 1 could provide the molecular basis for not only interpretation of physiological mechanisms in ATL or HAM/TSP but also development of novel therapeutic agents for HTLV-1–associated diseases.

CAN2 belongs to a Ca^{2+}-regulated cytosolic cysteine protease family, which includes 14 calpain isoforms.[26] The enzymatic activity of calpain is implicated in diverse physiological processes, such as cytoskeletal remodeling, cellular signaling, and apoptosis.[26] As an example of a spectrin-mediated apoptosis pathway, it was reported that CAN2 produced SPTA2 breakdown products following traumatic brain injury.[27] Because SPTA2 interacts with calmodulin and constructs the membrane cytoskeletons, its breakdown is considered a process of membrane structural changes during cell death.[28,29] This fact is concordant with our finding in ATL, suggesting that accumulation of SPTA2 in ATL cells can be attributed to the suppression of CAN2 expression and contribute to circumvent apoptosis. In the analysis of basal levels of CAN2 and SPTA2 in 7 cell lines (supplemental Figure 7), 3 ATL cell lines showed endogenous expression of CAN2 and moderate levels of SPTA2. On the other hand, 4 non-ATL leukemia cells demonstrated very high expression of SPTA2 and undetectable levels of CAN2. Although we found the downregulation of CAN2 and accumulation of SPTA2 in ATL cells, this tendency might be more distinctive in HTLV-1 (–) leukemia cells. Taken together, even though the expression level of CAN2 was indeed suppressed in ATL cells, the CAN2-SPTA2 apoptotic pathway itself might remain normal. In contrast, this pathway was considered to be impaired at multiple stages in HTLV-1 (–) leukemia cells because CAN2 expression was completely diminished (supplemental Figure 7) and overexpression of CAN2 could not reactivate the CAN2-SPTA2 apoptotic pathway (Figure 5B-E). In these cells, not only genetic downregulation of CAN2 but also inhibition of CAN2 enzymatic activity might be involved in the carcinogenesis.

In conclusion, comprehensive proteomic profiling of HTLV-1–infected T cells provided 17 disease-associated signature proteins, which have great potential for future clinical use as diagnostic biomarkers. As we described regarding the relationship between the CAN2-SPTA2 pathway and ATL phenotypes, further individual functional analyses will contribute to understanding the detailed molecular mechanisms involved in the onset or progression of HAM/TSP and ATL.

Acknowledgments

The authors thank Dr Hiroyuki Sorimachi for kindly providing pBlueBacIIICAPN2 vector.

This work was supported by Research on Measures for Intractable Diseases, the Ministry of Health Labour and Welfare Japan.

Authorship

Contribution: M.I. and K.U. designed the study, performed experiments, analyzed results, and wrote the manuscript; A.T. and N.S. performed experiments; N.A., T.S., A.U., and Y.Y. collected the clinical samples and performed flow cytometric experiments; Y.N. and H.N. revised the manuscript; and all authors discussed the results and commented on the manuscript.

Conflict-of-interest disclosure: The authors declare no competing financial interests.

Correspondence: Koji Ueda, Laboratory for Biomarker Development, Center for Genomic Medicine, RIKEN, General Research Building 6F, Institute of Medical Science, 4-6-1 Shirokanedai, Minato-ku, Tokyo, Japan, 1088639; e-mail: k-ueda@riken.jp.

References

1. Yamashita M, Ido E, Miura T, Hayami M. Molecular epidemiology of HTLV-I in the world. *J Acquir Immune Defic Syndr Hum Retrovirol.* 1996;13(suppl 1):S124-S131.
2. Asquith B, Zhang Y, Mosley AJ, et al. In vivo T lymphocyte dynamics in humans and the impact of human T-lymphotropic virus 1 infection. *Proc Natl Acad Sci U S A.* 2007;104(19):8035-8040.
3. Sakashita A, Hattori T, Miller CW, et al. Mutations of the p53 gene in adult T-cell leukemia. *Blood.* 1992;79(2):477-480.
4. Beltran B, Quiñones P, Morales D, Cotrina E, Castillo JJ. Different prognostic factors for survival in acute and lymphomatous adult T-cell leukemia/lymphoma. *Leuk Res.* 2011;35(3):334-339.
5. Ishida T, Joh T, Uike N, et al. Defucosylated anti-CCR4 monoclonal antibody (KW-0761) for relapsed adult T-cell leukemia-lymphoma: a multicenter phase II study. *J Clin Oncol.* 2012; 30(8):837-842.
6. Semmes OJ, Cazares LH, Ward MD, et al. Discrete serum protein signatures discriminate between human retrovirus-associated hematologic and neurologic disease. *Leukemia.* 2005;19(7):1229-1238.
7. Kirk PD, Witkover A, Courtney A, et al. Plasma proteome analysis in HTLV-1-associated myelopathy/tropical spastic paraparesis. *Retrovirology.* 2011;8:81.
8. Rahman S, Quann K, Pandya D, Singh S, Khan ZK, Jain P. HTLV-1 Tax mediated downregulation of miRNAs associated with chromatin remodeling factors in T cells with stably integrated viral promoter. *PLoS ONE.* 2012;7(4):e34490.
9. Polakowski N, Gregory H, Mesnard JM, Lemasson I. Expression of a protein involved in bone resorption, Dkk1, is activated by HTLV-1 bZIP factor through its activation domain. *Retrovirology.* 2010;7:61.
10. Yamano Y, Araya N, Sato T, et al. Abnormally high levels of virus-infected IFN-gamma+ CCR4+ CD4+ CD25+ T cells in a retrovirus-associated neuroinflammatory disorder. *PLoS ONE.* 2009;4(8):e6517.
11. Oh JH, Gao J, Nandi A, Gurnani P, Knowles L, Schorge J. Diagnosis of early relapse in ovarian cancer using serum proteomic profiling. *Genome Inform.* 2005;16(2):195-204.
12. Anderson NL, Anderson NG. The human plasma proteome: history, character, and diagnostic prospects. *Mol Cell Proteomics.* 2002;1(11): 845-867.
13. Nordon IM, Brar R, Hinchliffe RJ, Cockerill G, Thompson MM. Proteomics and pitfalls in the search for potential biomarkers of abdominal aortic aneurysms. *Vascular.* 2010;18(5):264-268.
14. Ueda K, Katagiri T, Shimada T, et al. Comparative profiling of serum glycoproteome by sequential purification of glycoproteins and 2-nitrobenzensulfenyl (NBS) stable isotope labeling: a new approach for the novel biomarker discovery for cancer. *J Proteome Res.* 2007;6(9): 3475-3483.
15. Ueda K, Fukase Y, Katagiri T, et al. Targeted serum glycoproteomics for the discovery of lung cancer-associated glycosylation disorders using lectin-coupled ProteinChip arrays. *Proteomics.* 2009;9(8):2182-2192.
16. Ueda K, Takami S, Saichi N, et al. Development of serum glycoproteomic profiling technique; simultaneous identification of glycosylation sites and site-specific quantification of glycan structure changes. *Mol Cell Proteomics.* 2010;9(9): 1819-1828.
17. Ueda K, Saichi N, Takami S, et al. A comprehensive peptidome profiling technology for the identification of early detection biomarkers for lung adenocarcinoma. *PLoS ONE.* 2011;6(4): e18567.
18. Bahbouhi B, al-Harthi L. Enriching for HIV-infected cells using anti-gp41 antibodies indirectly conjugated to magnetic microbeads. *Biotechniques.* 2004;36(1): 139-147.
19. Matsubar Y, Hori T, Morita R, Sakaguchi S, Uchiyama T. Delineation of immunoregulatory properties of adult T-cell leukemia cells. *Int J Hematol.* 2006;84(1):63-69.
20. Best I, López G, Verdonck K, et al. IFN-gamma production in response to Tax 161-233, and frequency of CD4+ Foxp3+ and Lin HLA-

DRhigh CD123+ cells, discriminate HAM/TSP patients from asymptomatic HTLV-1-carriers in a Peruvian population. *Immunology.* 2009; 128(1, pt 2):e777-e786.

21. Nakamura N, Fujii M, Tsukahara T, et al. Human T-cell leukemia virus type 1 Tax protein induces the expression of STAT1 and STAT5 genes in T-cells. *Oncogene.* 1999;18(17): 2667-2675.
22. Alaiya AA, Al-Mohanna M, Aslam M, et al. Proteomics-based signature for human benign prostate hyperplasia and prostate adenocarcinoma. *Int J Oncol.* 2011;38(4): 1047-1057.
23. Cappello F, Rappa F, David S, Anzalone R, Zummo G. Immunohistochemical evaluation of PCNA, p53, HSP60, HSP10 and MUC-2 presence and expression in prostate carcinogenesis. *Anticancer Res.* 2003;23(2B): 1325-1331.
24. Letsas KP, Vartholomatos G, Tsepi C, Tsatsoulis A, Frangou-Lazaridis M. Fine-needle aspiration biopsy-RT-PCR expression analysis of prothymosin alpha and parathymosin in thyroid: novel proliferation markers? *Neoplasma.* 2007; 54(1):57-62.
25. Anderson DD, Quintero CM, Stover PJ. Identification of a de novo thymidylate biosynthesis pathway in mammalian mitochondria. *Proc Natl Acad Sci USA.* 2011;108(37): 15163-15168.
26. Storr SJ, Carragher NO, Frame MC, Parr T, Martin SG. The calpain system and cancer. *Nat Rev Cancer.* 2011;11(5):364-374.
27. Liu MC, Akle V, Zheng W, et al. Comparing calpain- and caspase-3-mediated degradation patterns in traumatic brain injury by differential proteome analysis. *Biochem J.* 2006;394(pt 3): 715-725.
28. Wallis CJ, Wenegieme EF, Babitch JA. Characterization of calcium binding to brain spectrin. *J Biol Chem.* 1992;267(7): 4333-4337.
29. Liu X, Van Vleet T, Schnellmann RG. The role of calpain in oncotic cell death. *Annu Rev Pharmacol Toxicol.* 2004;44: 349-370.

白血病
非定型白血病および特殊型

HTLV-1関連脊髄症(HAM)

HTLV-1-associated myelopathy(HAM)

Key words：HAM，疫学，診断，治療，予後

山野嘉久[1]
佐藤知雄[1]
宇都宮 與[2]

1. 概　　念

HTLV-1関連脊髄症(HTLV-1-associated myelopathy：HAM)は，成人T細胞性白血病リンパ腫(ATL)の原因ウイルスであるhuman T-lymphotropic virus type 1(HTLV-1)の感染者(キャリア)の一部に発症する，進行性の脊髄障害を特徴とする神経難病である．1986年に納らにより一つの疾患単位として提唱され[1]，2009年度からは国の難治性疾患克服研究事業の対象疾患(いわゆる難病)に認定されている．

2. 疫　　学

日本では，HTLV-1キャリアの生涯において約0.3％の確率で発症すると推定されている[2]．患者の分布は西日本を中心に全国に広がっており，特に九州・四国・沖縄に多く，ATLの分布と一致していた．最近の全国疫学調査では，全国の患者数は約3,000人と推定され，関東などの大都市圏で患者数が増加していることが明らかとなりつつある．

HTLV-1の感染経路として，主として母乳を介する母子感染と，輸血，性交渉による水平感染が知られているが，そのいずれでも発症することが知られている．輸血後数週間で発症した例もあり，感染成立後長期のキャリア状態を経て発症するATLとは異なっている．輸血後発症するHAMの存在の指摘により，1986年11月より献血時の抗HTLV-1抗体のスクリーニングが開始され，以後，輸血後発症はなくなった．発症は中年以降の成人が多いが(平均発症年齢は40歳代)，10歳代，あるいはそれ以前の発症と考えられる例も存在する．男女比は1：2と女性に多く，男性に多いATLと対照的である．

表1　HAMの初期症状

- 何となく歩きにくい，両下肢のつっぱり感，足がもつれる，つまずく，走ると転びやすい，などの歩行障害に関する症状
- 排尿障害や便秘も，早期から自覚されることが多く，尿閉や頻尿，繰り返す膀胱炎で泌尿器科を受診しHAMと診断されることもある
- まれに，持続する両下肢のしびれ感，痛みなどを早期から認めることがある

3. 診断と鑑別診断

HAMは，早期の診断と治療介入が重要で，病気を見逃さない注意が必要である．**表1**のような症状の患者を診たら，HAMという疾患を思い浮かべることが重要である．HAMを疑ったらすぐに神経内科医への紹介を考慮してほしい．症状や診察所見の組み合わせは特徴的であるので，神経内科医であれば診断は比較的容易であることが多い．

痙性対麻痺を呈しHAMの可能性が考えられる場合，血清中の抗HTLV-1抗体の有無をEIA法またはPA法でスクリーニングし，陽性の場

[1]Yoshihisa Yamano, [1]Tomoo Sato, [2]Atae Utsunomiya: [1]Department of Rare Diseases Research, Institute of Medical Science, St. Marianna University School of Medicine　聖マリアンナ医科大学 難病治療研究センター 病因・病態解析部門　[2]Department of Hematology, Imamura Bun-in Hospital　今村病院分院 血液内科

0047-1852/13/¥60/頁/JCOPY

合はウエスタンブロット法で確認，感染を確定する．感染が確認されたら髄液検査を施行し，髄液の抗HTLV-1抗体が陽性の場合，他のミエロパチーをきたす脊髄圧迫病変，脊髄腫瘍，多発性硬化症，視神経脊髄炎などを鑑別したうえで，HAMと確定診断する[3]．

4．症状・経過

臨床症状の中核は，緩徐進行性の両下肢痙性不全麻痺で，両下肢の筋力低下と痙性による歩行障害を示す．初期症状は，歩行の違和感，足のしびれ，つっぱり感，足がもつれる，転びやすいなどであるが，多くは進行し，片手杖，両手杖，更に車椅子が必要となり徐々に日常生活が困難になる．重症例では下肢の完全麻痺や体幹の筋力低下による座位保持困難により，寝たきりになる場合もある．感覚の異常は約6割に認められ，下半身の触覚や温痛覚の低下がみられることがある．持続するしびれ感や痛みなどを伴う場合もあり，特に痛みを伴う場合はQOL低下の主要な原因となる[4]．

自律神経症状は高率にみられ，特に排尿困難，頻尿，便秘などの膀胱直腸障害は病初期よりみられる．また進行例では起立性低血圧や下半身の発汗障害なども認められ，発汗低下によるうつ熱のため，夏場に微熱，倦怠感が続き，適切な室温管理が必要となることもある．そのほか男性ではインポテンツがしばしばみられる[4]．

神経内科学的診察では，両下肢の深部腱反射の亢進，腹壁反射の消失が認められる．またバビンスキー徴候などの病的反射が下肢でみられる[4]．

HAM患者の約8割は年単位で緩徐に慢性に進行するが(慢性進行例)，時に急速に進行し数カ月で歩行不能になる例もみられ(急速進行例)，特に高齢での発症者で進行度が早い傾向がある．一方で，運動障害が軽度のまま10年以上の長期にわたり症状の進行があまり認められない例もある(慢性軽症例)．このようにHAMの経過には個人差が大きいという特徴があり，その経過は疾患活動性(特に脊髄炎症)の程度と相関している場合が多いので，治療方針を決定するうえでこれらの特徴を考慮する必要がある．

5．病因・病態

1）病　　理

HAMの病態を理解するうえで，病理所見を理解することは重要である．HAMの剖検例では，肉眼的に頸髄下部から腰髄上部までびまん性の萎縮がみられる．脊髄の横断面では両側側索の萎縮と変性が肉眼的に観察される．HAMの病理組織所見では，慢性炎症過程が脊髄，特に胸髄中・下部に強調されて起こっている．病変はほぼ左右対称性で，小血管周囲から脊髄実質に広がる炎症細胞浸潤と周囲の脊髄実質，すなわち，髄鞘や軸索の変性脱落がみられる．主として両側側索に強くみられ，灰白質にも及んでいる[5]．その他の詳細な解析も含めて，HAM患者脊髄では細胞性免疫反応が持続的に起こっていることを示す所見が得られている．更にHAMの脊髄病変において，HTLV-1感染細胞について*in situ* PCR法を用いて解析されており，HTLV-1の感染は浸潤したT細胞にのみ確認され，周辺の神経細胞やグリア細胞には確認されていない[6]．このことは，浸潤したHTLV-1感染T細胞が慢性炎症の要因として中心的な役割を果たしていることを示唆している．

2）ウイルス免疫学的な特徴

HAM患者では，末梢血単核球(PBMC)中のプロウイルス量，すなわち感染細胞数が健常キャリアに比較して有意に多いことが判明している[7]．また，ウイルス感染細胞に反応するHTLV-1特異的細胞傷害性T細胞や抗体の量も異常に増加しており，ウイルスに対する免疫応答が過剰に亢進しているという免疫学的な特徴を有している[8]．更に，髄液中や脊髄病変局所で一部の炎症性サイトカインやケモカインの産生が非常に高まっていることが知られている[9]．これらのウイルス・免疫学的特徴と病理学的な所見などを総合すると，HAMの主要な病態は，①HTLV-1感染細胞の増加と活性化，②脊髄の慢性炎症，③脊髄組織の破壊と変性，と考えられる．

6. HAMの検査

HAM患者の検査では，抗HTLV-1抗体価が健常キャリアやATL患者に比して高値のことが多い．また，HAMでは血清中の可溶性IL-2受容体濃度が高いことが多く，末梢レベルでのウイルスに起因する免疫応答の亢進を非特異的に反映しているものと考えられる．髄液所見は脊髄での炎症の程度を把握するうえで極めて重要である．軽度の細胞数，タンパク，IgGの増加がみられることがあり，急速進行例では高い値を示す傾向がある[9]．ただし，一般的な髄液検査で把握できるこれらの検査項目では，HAMの炎症を把握するには感度が低く，実際は炎症があり症状が進行性であってもこれらの値は正常範囲内にとどまることがあるので注意が必要である．現時点では，髄液中のネオプテリン濃度が保険未承認であるが外注検査可能であり，重症度との相関性もかなり高く，HAMの疾患活動性や治療効果の把握に有用である．PBMC中のプロウイルス量の定量測定値は，ウイルス感染症としての制御具合を把握することが可能となる．疾患活動性との相関は髄液の炎症所見ほど強くないが，HAM患者の長期予後との相関性が疫学的に証明されており[10]，将来，本格的なHTLV-1感染細胞の制御治療薬が出現した場合，重要な指標となることが考えられる．現在，厚生労働省研究班でHTLV-1ウイルス量測定法の標準化に向けた研究が実施されており，将来保険承認されることが期待される．

画像診断ではMRIで通常，胸髄を中心にびまん性に萎縮した像が得られ，局所性病変は一般的にはみられないが，発症後間もない症例で頸髄や胸髄でのびまん性の腫大やT2強調画像での髄内の強信号像が報告されている[11]．

7. 治療と予後

1) 治療の考え方

HAMは，その経過や疾患活動性の個人差が大きいという特徴があるので，それを踏まえた治療方針の決定が必要である．すなわち，できるだけ発症早期に，将来重症化する可能性があるか疾患活動性を判定し，その程度に応じて治療内容を検討することが望ましい．急速に進行して髄液の炎症所見が強い症例の場合は，比較的強い治療が初期に必要となる場合が多い．治療にはwindow of opportunityが存在し，治療によって改善が見込める時期を逃さないことが求められる．一方，ほとんど進行が認められず髄液の所見もおとなしい症例の場合は，副作用の強い治療薬の必要性に乏しい．HAMに最も多い緩徐に進行する症例の場合は，髄液の炎症所見や臨床経過などから活動性か非活動性であるかを判断し，治療内容を決定していく必要がある．

2) HAMの病態に則した治療戦略

前述したようにHAMの病態は，脊髄におけるHTLV-1感染細胞に起因した慢性炎症による神経組織障害とされている．よってその治療には①HTLV-1感染細胞の排除，②脊髄炎症の鎮静化，③神経細胞の再生が必要であるが，現時点では抗ウイルス療法や神経再生治療は研究段階であり，HAMの治療は炎症抑制効果をもつ副腎皮質ステロイド(ステロイド)と，免疫調整・抗ウイルス作用をもつインターフェロンα(IFN-α)による治療が主である．

ステロイド治療は，HAMに対する有効率および即効性に優れている．プレドニゾロン(PSL)は最も使用された実績があり多くの後ろ向き研究があるが，規模の大きなものではHAM 200例のレトロスペクティブな解析で，131人の患者にPSLの内服が試みられ，81.7％に有効，69.5％に著効し，同じ報告でIFN-αは32人の患者で62.5％に有効，21.9％に著効を示している[12]．このことはHAMの病態に炎症が深くかかわっており，その適切な制御・調節がHAMに有効であることを示している．しかしながら，長期にわたるステロイド治療の継続は，肥満，糖尿病，骨粗鬆症，白内障，感染症の誘発などの副作用を出現させる恐れがあるので，髄液の炎症所見や臨床的な治療反応性，年齢などを考慮し，できるだけ内服量を少なくする努力が必要である．なお，PSL治療によりウイルス量が増加することはない．

IFN-αは，多施設無作為抽出二重盲検法での治験が行われ，計48人の患者で28日間毎日注射療法を行った場合に用量依存的に効果を有することが報告された[13]．現在HAMに対する保険承認を得ている唯一の薬剤である．IFN-αのHAMへの治療効果のメカニズムは必ずしも明らかではないが，治療後ウイルス量が若干減少していること，HAMでみられる免疫異常が改善していることなどから，抗ウイルス作用と免疫調整作用の両者が関与していると推定される．欠点は，PSLに比較して抗炎症効果・即効性に乏しいこと，効果発現に週3回以上の注射施行を必要とするため長期間の治療継続が困難な場合が多い点である．また，主な副作用として，発熱・全身倦怠感・食欲不振などのインフルエンザ様症状，脱毛，間質性肺炎，抑うつ，血球減少などがある．

HAMの治療の最終目標は長期予後の改善である．PSLもIFN-αも長期予後改善効果に関するエビデンスに乏しい．また，PSL長期内服は副作用の問題があり，また現行のIFN-α注射療法も長期治療継続は困難で，これらの治療薬の長期使用患者は限定されるのが現状であり，より効果や長期忍容性に優れた新規治療薬開発の要望が強い．

HAMの治療として免疫抑制作用薬剤による脊髄炎症の鎮静化が重要であることは明らかであるが，HAMはウイルス感染症ならびにATL発症リスクを抱えるという特徴があり，これらを意識した新薬開発も重要と考えられている．HAMに対する抗ウイルス療法としては，逆転写酵素阻害剤を用いた臨床試験が報告されているが，ウイルス量の減少効果は全く得られていない[14]．HTLV-1はエイズウイルスとは異なり血清中でウイルスが存在せず転写レベルが低いという特徴を有しているので，ウイルス量の制御には異なった戦略が必要であると考えられる．最近，ATLにおいて抗CCR4抗体療法が保険承認されており，CCR4はHAMにおける感染細胞のマーカーとしても有用であるので[15]，今後の結果に注目したい．

3）HAMの随伴症状に対する治療

筋力維持や痙性緩和のための継続的なリハビリや，痙性や疼痛に対する抗痙縮薬や中枢性鎮痛剤の投与など，HAMの諸症状に対する対症療法は，ADL維持のために非常に重要である．また重度の排尿障害に対する自己導尿や，ぶどう膜炎や肺胞炎，褥瘡などの合併症検索など他科と連携をとりながら，きめ細かい治療を行うことが望まれる．

文　献

1) Osame M, et al: HTLV-I associated myelopathy, a new clinical entity. Lancet 1(8488): 1031-1032, 1986.
2) Kaplan JE, et al: The risk of development of HTLV-I-associated myelopathy/tropical spastic paraparesis among persons infected with HTLV-I. J Acquir Immune Defic Syndr 3(11): 1096-1101, 1990.
3) World Health Organization(WHO): Human T lymphotropic virus type 1, HTLV-1. Wkly Epidemiol Rec 64: 382-383, 1989.
4) Nakagawa M, et al: HTLV-I-associated myelopathy: analysis of 213 patients based on clinical features and laboratory findings. J Neurovirol 1(1): 50-61, 1995.
5) Izumo S, et al: HTLV-I-associated myelopathy. Neuropathology 20: S65-S68, 2000.
6) Matsuoka E, et al: Perivascular T cells are infected with HTLV-I in the spinal cord lesions with HTLV-I-associated myelopathy/tropical spastic paraparesis: double staining of immunohistochemistry and polymerase chain reaction in situ hybridization. Acta Neuropathol 96(4): 340-346, 1998.
7) Nagai M, et al: Analysis of HTLV-I proviral load in 202 HAM/TSP patients and 243 asymptomatic HTLV-I carriers: high proviral load strongly predisposes to HAM/TSP. J Neurovirol 4(6): 586-593, 1998.
8) Jacobson S: Immunopathogenesis of human T cell lymphotropic virus type I-associated neuro-